Chemistry of bis(dialkoxyphosphino)methylamines. Mono- and bimetallic complexes of chromium(0), molybdenum(0), tungsten(0), rhodium(I), and ruthenium(II)

Joel T. Mague, and M. Pontier Johnson

Organometallics, **1990**, 9 (4), 1254-1269• DOI: 10.1021/om00118a057 • Publication Date (Web): 01 May 2002

Chemistry of Bis(dialkoxyphosphino)methylamines. Mono- and Bimetallic Complexes of Chromium(0), Molybdenum(0), Tungsten(0), Rhodium(I), and Ruthenium(II)

Joel T. Mague* and M. Pontier Johnson

Department of Chemistry, Tulane University, New Orleans, Louisiana 70118

Received November 21, 1989

The ligating behavior of the "short-bite" ligands $CH_3N(P(OR_2)_2$ (R = CH_3 (L_2), *i*-C_3H_7 (L_2'), CH_2– (L_2'')) has been investigated. With $[M(CO)_3(\eta^6\text{-}C_7H_8)]$ (M = Cr, Mo, W) the primary products are the ligand-bridged dimers $[M_2(CO)_6(CH_3N(P(OR)_2)_2)_2(\mu\text{-}CH_3N(P(OR)_2)_2)]$, which have been obtained as all-mer, all-fac, and mer-fac isomers depending on the ligand and conditions used. With an excess of L_2', *mer*-$[Mo(CO)_3(\eta^2\text{-}L_2')(\eta^1\text{-}L_2')]$ could be obtained in high yield and was used to prepare heterobimetallic complexes $[MoM(CO)_4Cl(L_2')_2]$ (M = Rh (**20**), Ir (**21**)). Low yields of *mer*-$[M(CO)_3(\eta^2\text{-}L_2)(\eta^1\text{-}L_2)]$ and *mer*-$[M(CO)_3(\eta^2\text{-}L_2')(\eta^1\text{-}L_2')]$ (M = Cr, W) were also obtained. Attempts to prepare related ruthenium complexes were unsuccessful, and only $[(\eta^5\text{-}C_5H_5)RuCl(L_2)]$ (**27**) was obtained. The ligand L_2' is evidently too bulky to form dimeric complexes with rhodium as the product isolated was $[Rh(L_2')_2]ClO_4$. An interesting minor product obtained during the synthesis of *mer*-$[W_2(CO)_6(L_2)_2(\mu\text{-}L_2)]$ was shown to be $[W_2(CO)_6(CH_3N(P(OCH_3)_2)_2)(CH_3OP(N(CH_3)P(OCH_3)_2)_2)]$ (**16**), which contains a bridging tridentate ligand, a semibridging carbonyl group, and possibly a metal–metal bond. The ^{31}P NMR spectra of the group VI metal complexes are discussed. The structures of *mer*-$[W_2(CO)_6(L_2)_2(\mu\text{-}L_2)]$ (**12**), **16**, **20**, **21**, and **27** have been determined by X-ray crystallography. **12**: monoclinic, $P2_1/c$, a = 17.421 (3), b = 15.581 (5), c = 17.116 (6) Å, β = 117.26 (2)°, Z = 4, 4282 data ($I \geq 3\sigma(I)$), R = 0.035, R_w = 0.044. **16**: orthorhombic, $P2_12_12_1$, a = 14.512 (3), b = 15.202 (4), c = 15.577 (3) Å, Z = 4, 2233 data ($I \geq 3\sigma(I)$), R = 0.031, R_w = 0.037. **20**: orthorhobmic, $Pna2_1$, a = 16.561 (4), b = 12.964 (3), c = 21.530 (5) Å, Z = 4, 2685 data ($I \geq 2\sigma(I)$), R = 0.045, R_w = 0.054. **21**: orthorhombic, $Pna2_1$, a = 16.545 (3), b = 12.921 (2), c = 21.595 (5) Å, Z = 4, 2923 data ($I \geq 3\sigma(I)$), R = 0.040, R_w = 0.053. **27**: monoclinic, $P2_1/n$, a = 7.6964 (8), b = 8.8436 (6), c = 23.8778 (23) Å, β = 96.856 (8)°, Z = 4, 2791 data ($I \geq 3\sigma(I)$), R = 0.026, R_w = 0.039.

Introduction

The "short-bite" ligands $(R_2P)_2CH_2$ (R = Me (dmpm), Ph (DPPM)) have long been known to form a variety of homo and heterobimetallic complexes[1-5] as well as some with higher nuclearity.[6-9] More recently, the geometrically similar ligands $RN(PX_2)_2$ (R = alkyl; X = F, alkoxy, phenoxy) have received sporadic study. In addition to routine complexes[10,11] and analogues of some dmpm and DPPM dimers,[12] $CH_3N(P(OCH_3)_2)_2$[13,14] and particularly $CH_3N(PF_2)_2$[15-20] have been found to form a number of complexes with unusual and unexpected structures. As part of our continuing interest in polynuclear complexes of "short-bite" ligands, we have undertaken an extensive study of the ligating properties of $RN(PX_2)_2$. Previously we have reported the synthesis of the novel species $[Rh_2(CH_3N(P(OCH_3)_2)_2)_2(\mu\text{-}CH_3N(P(OCH_3)_2)_2)_2]X_2$ (X = BPh_4, ClO_4, PF_6, CF_3SO_3)[13] and $[Rh_3(\mu\text{-}Cl)_3(\mu\text{-}CH_3N(PF_2)_2)_3]$[15] and now describe further chemistry of the $CH_3N(P(OR)_2)_2$ (R = Me, Pr^i, CH_2–) ligands including the synthesis of several heterobimetallic complexes.

Experimental Section

All reactions were carried out under an atmosphere of purified nitrogen using standard Schlenk techniques. Solvents were purified by standard methods and distilled under nitrogen from appropriate drying agents prior to use. Literature methods were used to prepare $[MCl(COD)]_2$ (M = Rh,[13] Ir;[21] COD = cycloocta-1,5-diene), $[M(CO)_3(CHT)]$ (M = Cr,[22a] Mo,[22b] W;[23] CHT = cyclohepta-1,3,5-triene), $[W(CO)_4(NBD)]$[23] (NBD = bicyclo[2.2.1]heptadiene), $[CpRu(COD)Cl]$,[24] $[(C_6H_5)_2P]_2CHC_5H_4N$,[25] $CH_3N(PCl_2)_2$,[11] and $CH_3N(P(OCH_3)_2)_2$.[11] ^1H and $^{31}P\{^1H\}$ NMR spectra were obtained on an IBM-Brucker AF-200 spectrometer at 200.132 and 81.015 MHz, respectively. Proton and phosphorus chemical shifts are respectively referred to tetramethylsilane (δ 0.0) and 85% H_3PO_4 (δ 0.0) as external standards employing the

(1) Puddephatt, R. J. *Chem. Soc. Rev.* **1983**, *12*, 99.
(2) Chaudret, B.; Delavaux, B.; Poilblanc, R. *Coord. Chem. Revs.* **1988**, 86, 191.
(3) Jenkins, J. A.; Ennett, J. P.; Cowie, M. *Organometallics* **1988**, *7*, 1845, and references therein.
(4) Lemke, F. R.; De Laet, D. L.; Gao, J.; Kubiak, C. P. *J. Am. Chem. Soc.* **1988**, *110*, 6904, and references therein.
(5) Fontiane, X. L. R.; Jacobsen, G. B.; Shaw, B. L. *J. Chem. Soc., Dalton Trans.* **1988**, 2235, and references therein.
(6) Jennings, M. C.; Manojlovic-Muir, L.; Puddephatt, R. J. *J. Am. Chem. Soc.* **1988**, *111*, 745, and references therein.
(7) Ramachandran, R.; Payne, N. C.; Puddephatt, R. J. *J. Chem. Commun.* **1988**, 128.
(8) Hadj-Bagheri, N.; Puddephatt, R. J. *Inorg. Chem.* **1989**, *28*, 2384.
(9) Braunstein, P.; Luke, M. A.; Tiripicchio, A.; Camellini, M. T. *Nouv. J. Chem.* **1988**, *12*, 429.
(10) Brown, G. M.; Finholt, J. E.; King, R. B.; Bibber, J. W.; Kim, J. H. *Inorg. Chem.* **1982**, *21*, 3790.
(11) Brown, G. M.; Finholt, J. E.; King, R. B.; Bibber, J. W. *Inorg. Chem.* **1982**, *21*, 2139.
(12) Field, J. S.; Haines, R. J.; Sampson, C. N. *J. Chem. Soc., Dalton Trans.* **1987**, 1933, and references therein.
(13) Mague, J. T.; Lloyd, C. L. *Organometallics* **1988**, *7*, 983.
(14) Mague, J. T. *Inorg. Chem.* **1989**, *28*, 2215.
(15) Mague, J. T.; Johnson, M. P.; Lloyd, C. L. *J. Am. Chem. Soc.* **1989**, *111*, 5012.
(16) Mague, J. T.; Johnson, M. P. *Acta Crystallogr.* **1990**, *C46*, 129.
(17) Dulebohn, J. I.; Ward, D. L.; Nocera, D. G. *J. Am. Chem. Soc.* **1988**, *110*, 4054.
(18) King, R. B.; Shimura, M.; Brown, G. M. *Inorg. Chem.* **1984**, *23*, 1398.
(19) Newton, M. G.; King, R. B.; Chang, M.; Pantaleo, N. S.; Gimeno, J. *J. Chem. Soc., Chem. Commun.* **1977**, 531.
(20) Newton, M. G.; King, R. B.; Lee, T.-W.; Norskov-Lauritzen, L.; Kumar, V. *J. Chem. Soc., Chem. Commun.* **1982**, 201.
(21) Crabtree, R. H.; Quirk, J. M.; Felkin, H.; Fillebeen-Khan, T. *Synth. React. Inorg. Met.-Org. Chem.* **1982**, *12*, 407.
(22) King, R. B. *Organometallic Syntheses*; Academic Press: New York, 1965; Vol. 1, (a) p 123, (b) p 125.
(23) King, R. B.; Fronzaglia, A. *Inorg. Chem.* **1966**, *5*, 1837.
(24) Albers, M. O.; Robinson, D. J.; Shaver, A.; Singleton, E. *Organometallics* **1986**, *5*, 2199.
(25) Anderson, M. P.; Mattson, B. M.; Pignolet, L. H. *Inorg. Chem.* **1983**, *22*, 2644.

0276-7333/90/2309-1254$02.50/0

high-frequency-positive convention. Spectral simulations were performed using the PANIC portion of the IBM Aspect-3000 software. Infrared spectra were obtained on a Mattson-Cygnus 100 Fourier transform spectrometer. Microanalyses were performed by Galbraith Laboratories, Knoxville, TN.

$CH_3N(P(OCH(CH_3)_2)_2)_2$. By analogy with the synthesis of $CH_3N(P(OCH_3)_2)_2$, a mixture of 76.4 g (105.6 mL, 0.754 mol) of triethylamine and 45.3 g (57.7 mL, 0.754 mol) of dry propan-2-ol was added dropwise to a mechanically stirred solution of 43.9 g (0.188 mol) of $CH_3N(PCl_2)_2$ in 1000 mL of dry diethyl ether at −78 °C. After completion of the addition the reaction mixture was allowed to warm to room temperature and was filtered to remove precipitated triethylammonium chloride. The solvents were removed by distillation at atmospheric pressure, and the residue was fractionated at reduced pressure. The product was obtained as a colorless liquid (bp 90 °C, 0.6 mmHg; yield 23.1 g (38%)): ^{1}H NMR ($CDCl_3$) δ 4.09 (sd, 4 H, $OCH(CH_3)_2$), 2.48 (t (J = 3.3 Hz), 3 H, NCH_3), 1.20 (d (J = 6.2 Hz), 12 H, $OCH(CH_3)_2$), 1.16 (d (J = 6.2 Hz), 12 H, $OCH(CH_3)_2$); $^{31}P\{^1H\}$ NMR ($CDCl_3$) δ 139.4 (s).[26]

$CH_3N(POCH_2CH_2O)_2$. To a solution of 76.4 g (105.6 mL, 0.754 mol) of triethylamine in 1500 mL of dry diethyl ether at −78 °C was added dropwise and simultaneously from separate funnels 47.3 g (0.202 mol) of $CH_3N(PCl_2)_2$ in 20 mL of diethyl ether and 23.4 g (21 mL, 0.376 mol) of anhydrous ethylene glycol partially dissolved in 10 mL of diethyl ether and 10 mL of dichloromethane. During the addition the mixture was mechanically stirred, and at the end an additional 15 mL of triethylamine was added. Following warmup to ambient temperature the precipitated triethylammonium chloride was filtered off and washed with dichloromethane. The filtrate and washings were combined, and the solvents distilled off at atmospheric pressure until crystals formed. After sitting at room temperature overnight, the supernatant was removed with a syringe, and the crystals were washed with hexane and dried in vacuo. Concentration of the filtrate yielded additional product, which was similarly washed and dried. The extremely hygroscopic product was obtained as colorless crystals (25 g, 58%; mp 106–109 °C (lit. mp 103–105 °C)[27]): ^{1}H NMR ($CDCl_3$) δ 4.18–3.89 (m, 8 H, OCH_2CH_2O), 2.42 (t (J = 3.6 Hz), 3 H, NCH_3); $^{31}P\{^1H\}$ NMR ($CDCl_3$) δ 140.6 (s).

***mer*-$[Mo_2(CO)_6(CH_3N(P(OCH_3)_2)_2)_2(\mu\text{-}CH_3N(P(OCH_3)_2)_2)]$ (1a).** A solution of 0.5 g (1.84 mmol) of $[Mo(CO)_3(CHT)]$ and 0.593 g (2.76 mmol) of $CH_3N(P(OCH_3)_2)_2$ in 10 mL of toluene was heated at 60 °C for 3 h. The dark brown-yellow solution was filtered and evaporated to dryness in vacuo. The residue was extracted with 20 mL of hexane, and the remaining solid taken up in diethyl ether and filtered through a 5 × 2 cm column of alumina (Brockman II). Concentration of the filtrate under pressure and dilution with hexane afforded the product as pale yellow, somewhat air-sensitive crystals in 70% yield. Anal. Calcd for $C_{21}H_{45}O_{18}P_6N_3Mo_2$: C, 25.08; H, 4.52; N, 4.18. Found: C, 24.5; H, 4.5; N, 4.1. IR (toluene solution) 1983 (m), 1901 (s), 1890 (sh) cm^{-1} ($\nu_{C\equiv O}$);[28] ^{1}H NMR (C_6D_6) δ 3.72 (d, J = 12.1 Hz), 3.53 (d, J = 13.9 Hz), 3.49 (d, J = 13.2 Hz), (36 H, OCH_3), 3.00 (t (J = 10.6 Hz), 3 H, NCH_3 (bridge)), 2.39 (t (J = 8.6 Hz), 6 H, NCH_3 (chelate)); $^{31}P\{^1H\}$ NMR (C_6D_6) δ(P_1) 191.1, δ(P_2) 160.2, δ(P_3) 147.1 (J_{12} = 161.3, J_{13} = 46.6, J_{23} = 59.5, $J_{11'}$ = 16.2 Hz).[29]

The same product was obtained when a ligand:metal ratio of 2:1 was used.

***fac*- and *fac-mer*-$[Mo_2(CO)_6(CH_3N(P(OCH_3)_2)_2)_2(\mu\text{-}CH_3N(P(OCH_3)_2)_2)]$ (1b, 1c).** Dropwise addition of a hexane solution of 0.632 g (2.94 mmol) of $CH_3N(P(OCH_3)_2)_2$ to a stirred solution of 0.40 g (1.47 mmol) of $[Mo(CO)_3(CHT)]$ in 30 mL of hexane resulted in the precipitation of a pale yellow solid after 10 min. This was collected and recrystallized from toluene/hexane to give off-white crystals in 90% yield. The components of the isomeric mixture were identified from their ^{31}P NMR spectra; ^{1}H NMR (C_6D_6) (**1b**) δ 3.70 (d, J = 11.6 Hz), 3.54 (m), 3.31 (m), (OCH_3) 3.03 (t (J = 10.6 Hz), NCH_3 (bridge)), 2.41 (t (J = 8.3 Hz), NCH_3 (chelate)); (**1c**) δ 3.75 (d (J = 11.4 Hz)), 3.69 (d (J = 12.1 Hz)), 3.56 (m), 3.54 (d (J = 13.8 Hz)), 3.49 (d (J = 13.2 Hz)), 3.32 (m, OCH_3), 3.06 (t (J = 10.6 Hz), NCH_3 (bridge)), 2.42 (t (J = 8.1 Hz)), 2.40 (t (J = 8.6 Hz), NCH_3 (chelate)); $^{31}P\{^1H\}$ NMR (C_6D_6) (**1b**) δ(P_1) 177.0, δ(P_2) 145.9 (J_{12} = 42.4, $J_{11'}$ = 18.7, $J_{22'}$ = 69.3 Hz); (**1c**) δ(P_1) 190.2 (ddd), δ(P_2) 178.2 (td), δ(P_3) 146.3 (d), δ(P_4) 159.9 (dd), δ(P_5) 146.7 (dd) (J_{12} = 18.1, J_{14} = 161.7, J_{15} = 46.8, J_{23} = 42.0, J_{45} = 57.8 Hz).

***mer*-$[Mo_2(CO)_6(CH_3N(P(OCH(CH_3)_2)_2)_2)_2(\mu\text{-}CH_3N(P(OCH(CH_3)_2)_2)_2)]$ (2).** A solution of 0.40 g (1.47 mmol) of $[Mo(CO)_3(CHT)]$ and 0.722 g (2.205 mmol) of $CH_3N(P(OCH(CH_3)_2)_2)_2$ in 15 mL of toluene was heated at 60 °C for 3 h. Solvent was removed from the dark yellow-brown solution in vacuo, and the resulting oil taken up in hexane and placed on a column of alumina (Brockman III, 1 × 10 cm). The column was washed with hexane and then eluted with 1:9 diethyl ether/hexane to give a dark yellow-brown solution which yielded an oil upon removal of solvent. On standing at room temperature for two weeks, pale yellow air-sensitive crystals formed in the oil. The residual oil was removed via syringe, and the crystals were washed quickly with 5 mL of hexane and dried in vacuo. Although apparently a single species by ^{31}P NMR, satisfactory elemental analyses could not be obtained; IR (hexane solution) 1980 (m), 1884 (vs), 1870 (sh) cm^{-1} ($\nu_{C\equiv O}$); $^{31}P\{^1H\}$ NMR (hexane/acetone-d_6) δ(P_1) 189.8, δ(P_2) 153.4, δ(P_3) 136.5 (J_{12} = 163.4, J_{13} = 42.5, J_{23} = 69.1, $J_{11'}$ = 38.0 Hz).

***mer*-$[Mo(CO)_3(CH_3N(P(OCH(CH_3)_2)_2)_2)_2]$ (3).** A toluene solution (15 mL) of 0.40 g (1.47 mmol) of $[Mo(CO)_3(CHT)]$ and 0.962 g (2.94 mmol) of $CH_3N(P(OCH(CH_3)_2)_2)_2$ was heated at 60 °C for 2 h and then stirred at room temperature for a further 2 h. The solvent was removed from the brownish yellow solution in vacuo, and the residual oil taken up in hexane and chromatographed on alumina (Brockman III, 2 × 5 cm column). After development with hexane the column was eluted with diethyl ether/hexane (1:1) to remove a yellow band. Removal of the solvent gave the product as an orange-yellow, air-sensitive oil in 70% yield. The product was identified spectroscopically; IR (hexane solution) 1981 (vs), 1884 (vs), 1876 (sh) cm^{-1} ($\nu_{C\equiv O}$); ^{1}H NMR (C_6D_6) δ 4.91 (m), 4.68 (m), 4.2 (m, 8 H, $OCH(CH_3)_2$), 1.40–1.04 (m, 24 H, $OCH(CH_3)_2$), 2.90 (dd (J = 2.6, 11.6 Hz), 3 H, NCH_3 (η^1 ligand)), 2.47 (t (J = 8.5 Hz), 3 H, NCH_3 (η^2 ligand)); $^{31}P\{^1H\}$ NMR (C_6D_6) δ(P_1) 179.7 (ddd), δ(P_2) 151.1 (dd), δ(P_3) 138.1 (ddd), δ(P_4) 137.7 (dd) (J_{12} = 160.3, J_{13} = 42.9, J_{14} = 33.8, J_{23} = 68.1, J_{34} = 2.3 Hz).

***fac*-$[Mo_2(CO)_6(CH_3N(POCH_2CH_2O)_2)_2(\mu\text{-}CH_3N(POCH_2CH_2O)_2)]$ (4).** To a solution of 0.30 g (1.10 mmol) of $[Mo(CO)_3(CHT)]$ in 20 mL of diethyl ether was added 0.466 g (2.205 mmol) of solid $CH_3N(POCH_2CH_2O)_2$. After this was stirred for 10 min, a white, curdy precipitate formed, and the solution was pale pink. The solid was filtered off, washed with diethyl ether, and recrystallized from acetone/hexane as white crystals that are air sensitive and slowly acquire a tan cast on standing under nitrogen (yield 85%). Anal. Calcd for $C_{21}H_{33}O_{18}P_6N_3Mo_2$: C, 25.39; H, 3.36. Found: C, 25.3; H, 4.0. IR (Nujol mull) 1967 (s), 1865 (s) cm^{-1} ($\nu_{C\equiv O}$); ^{1}H NMR (acetone-d_6) δ 4.46–4.13 (m, 24 H, OCH_2CH_2O), 2.90 (t (J = 12.3 Hz), 3 H, NCH_3 (bridge)), 2.51 (t (J = 8.6 Hz), 6 H, NCH_3 (chelate)); $^{31}P\{^1H\}$ NMR (acetone-d_6) δ(P_1) 181.4, δ(P_2) 153.2 (J_{12} = 45.3, $J_{11'}$ = 26.0, $J_{22'}$ = 69.0 Hz).

***mer*-$[Cr_2(CO)_6(CH_3N(P(OCH_3)_2)_2)_2(\mu\text{-}CH_3N(P(OCH_3)_2)_2)]$ (5).** A solution of 0.30 g (1.315 mmol) of $[Cr(CO)_3(CHT)]$ and 0.424 g (1.972 mmol) of $CH_3N(P(OCH_3)_2)_2$ in 10 mL of hexane was refluxed overnight, by which time an off-white solid had formed and the solution was pale orange. The solution was syringed into a clean flask, and the solvent removed in vacuo. The residue was taken up in toluene and chromatographed on a 1 × 15 cm column of Brockman I alumina. Development with hexane followed by elution with toluene removed an orange band shown by ^{1}H NMR to be unreacted $[Cr(CO)_3(CHT)]$. Further elution with diethyl ether removed the product as a yellow band. Yellow

(26) Key to NMR peak multiplicities: s, singlet; d, doublet; t, triplet; q, quintet; m, multiplet; dd, doublet of doublets; td, triplet of doublets; sd, septet of doublets; ddd, doublet of doublets of doublets; sep, septet.

(27) Pudovik, M. A.; Medvedeva, M. D.; Pudovik, A. N. *Zh. Obshch. Khim.* **1976**, *46*, 773.

(28) Key to infrared band intensities: w, weak; m, medium; s, strong; vs, very strong; sh, shoulder.

(29) The numbering of phosphorus atoms, e.g., P_1, P_2, etc., for chemical shift assignments is that used in the drawings of the proposal structures. These appear in the Results. The coupling constants J_{ij} refer to $J_{P_i\text{-}P_j}$ using the same numbering system. Only $|J_{ij}|$ is given (see Discussion).

crystals could be obtained by recrystallization from diethyl ether/hexane (yield 15%). Anal. Calcd for $C_{21}H_{45}O_{18}P_6N_3Cr_2$: C, 27.49; H, 4.94; N, 4.58. Found: C, 26.6; H, 5.1; N, 4.8. IR (Nujol mull) 1971 (sh), 1962 (m), 1859 (vs), 1847 (sh) cm^{-1} ($\nu_{C\equiv O}$); ^1H NMR (C_6D_6) δ 3.77 (d (J = 11.5 Hz)), 3.58 (d (J = 13.0 Hz)), 3.53 (d (J = 12.4 Hz), 36 H, OCH_3), 3.01 (t (J = 10.0 Hz), 3 H, NCH_3 (bridge)), 2.40 (t (J = 9.05 Hz), 6 H, NCH_3 (chelate)); $^{31}P\{^1H\}$ NMR (C_6D_6) $\delta(P_1)$ 210.5, $\delta(P_2)$ 178.4, $\delta(P_3)$ 163.1 (J_{12} = 9.6, J_{13} = 63.9, J_{23} = 11.9, $J_{11'}$ = 16.7 Hz).

The original precipitate was recrystallized from toluene/hexane to afford a pale orange solid whose ^{31}P NMR spectrum indicated it to be impure **5**. This was not further investigated.

***mer*-[Cr(CO)$_3$(CH$_3$N(P(OCH$_3$)$_2$)$_2$)$_2$] (6).** This was identified spectroscopically as a minor component of the crude material obtained from the yellow, diethyl ether eluate described in the previous experiment; ^1H NMR (C_6D_6) δ 3.4–3.6 (m, OCH_3), 2.83 (dd (J = 2.5, 9.4 Hz), NCH_3 (η^1 ligand)), 2.39 (t (J = 9.12 Hz), NCH_3 (η^2 ligand)); $^{31}P\{^1H\}$ NMR (C_6D_6) $\delta(P_1)$ 210.5 (ddd), $\delta(P_2)$ 177.6 (dd), $\delta(P_3)$ 163.8 (ddd), $\delta(P_4)$ 144.8 (dd) (J_{12} = 11.3, J_{13} = 59.7, J_{14} = 77.8, J_{23} = 10.9, J_{34} = 9.1 Hz).

Reaction of [Cr(CO)$_3$(CHT)] with CH$_3$N(P(OCH(CH$_3$)$_2$)$_2$)$_2$. A diethyl ether solution (20 mL) of 0.25 g (1.096 mmol) of [Cr(CO)$_3$(CHT)] and 0.717 g (2.19 mmol) of $CH_3N(P(OCH(CH_3)_2)_2)_2$ was stirred at room temperature for 36 h with little evidence of reaction. The solvent was removed in vacuo and replaced with 20 mL of hexane, and the mixture refluxed overnight to yield a yellow solution and a green precipitate. The latter was removed by filtration, and the ^{31}P NMR spectrum of the filtrate indicated the presence of at least four species in addition to free ligand. The solution was concentrated under reduced pressure and chromatographed on a 1.5 × 20 cm column of Brockman III alumina. Elution with hexane removed two pale yellow fractions, and with 2:1 hexane/diethyl ether a further yellow band was obtained. The ^{31}P and ^1H NMR spectra of these fractions revealed that complete separation of the original mixture had not occurred. Further attempts to obtain pure compounds were unsuccessful; however, from the spectroscopic data, three products were identified as *mer*-[$Cr_2(CO)_6(CH_3N(P(OCH(CH_3)_2)_2)_2)_2(\mu$-$CH_3N$-$(P(OCH(CH_3)_2)_2)_2)$] (**7**), *mer*-[$Cr(CO)_3(CH_3N(P(OCH(CH_3)_2)_2)_2)_2$] (**8**), and *cis*-[$Cr(CO)_2(CH_3N(P(OCH(CH_3)_2)_2)_2)_2$] (**9**). IR (hexane solution) (**7**) 1968 (m), 1874 (vs), 1866 (sh) cm^{-1}; (**8**) 1968 (m), 1874 (vs), 1866 (sh) cm^{-1}; (**9**) 2017 (m), 1906 (s) cm^{-1} ($\nu_{C\equiv O}$); ^1H NMR (C_6D_6) (**7**) δ 2.36 (t (J = 9.4 Hz), N-CH_3 (bridge)), 2.49 (t (J = 4.6 Hz), N-CH_3 (chelate)); (**8**) δ 3.04 (dd (J = 11.4, 2.8 Hz), NCH_3 (η^1 ligand)), 2.47 (t (J = 8.9 Hz), NCH_3 (η^2 ligand)); (**9**) δ 2.50 (t (J = 9.0 Hz), NCH_3). The considerable overlap of the methine and the methyl proton resonances of the isopropoxy groups for the various species made assignments of these impossible. $^{31}P\{^1H\}$ NMR (C_6D_6) (**7**) $\delta(P_1)$ 190.2 (dd), $\delta(P_2)$ 171.6 (dd), $\delta(P_3)$ 156.1 (dd) (J_{12} = 18.1, J_{13} = 57.6, J_{23} = 20.1 Hz); (**8**) $\delta(P_1)$ 200.8 (ddd), $\delta(P_2)$ 171.4 (dd), $\delta(P_3)$ 154.6 (dd), $\delta(P_4)$ 138.0 (d) (J_{12} = 9.2, J_{13} = 56.1, J_{14} = 18.2, J_{23} = 18.2 Hz); (**9**) AA'XX', $\delta(P_A)$ 176.0, $\delta(P_X)$ 155.6, $J_{AA'}$ = 1.8, J_{AX} = 57.9, $J_{AX'}$ = −8.6, $J_{XX'}$ = 50.5 Hz).

***mer* and *fac*-*mer*-[Cr$_2$(CO)$_6$(CH$_3$N(POCH$_2$CH$_2$O)$_2$)$_2$(μ-CH$_3$N(POCH$_2$CH$_2$O)$_2$)] (10a, 10c).** A toluene solution (15 mL) of 0.461 g (2.184 mmol) of $CH_3N(POCH_2CH_2O)_2$ and 0.332 g (1.456 mmol) of [Cr(CO)$_3$(CHT)] was heated at 60 °C. After ca. 3 h a light-colored solid had begun to form. The reaction was terminated after 15 h, by which time considerable off-white solid was present and the solution was a pale orange–pink. After cooling, the liquid was removed via syringe, and the solid was washed with 5 mL of toluene and 8 mL of diethyl ether and dried in vacuo (yield 73%). From the ^{31}P NMR it was apparent that the product was an isomeric mixture. Anal. Calcd for $C_{21}H_{33}O_{18}P_6N_3Cr_2$: C, 27.86; H, 3.86; N, 4.64. Found: C, 27.6; H, 39; N, 4.5. ^1H NMR (**10a**) (acetone-d_6) δ 4.4–4.1 (m, OCH_2CH_2O), 2.82 (t (J = 11.8 Hz), NCH_3 (bridge)), 2.49 (t (J = 9.1 Hz), NCH_3 (chelate)); (**10c**) ($CDCl_3$) δ 4.2–4.1 (m, OCH_2CH_2O), 2.59 (t (J = 10.1 Hz), NCH_3 (bridge)), 2.44 (t (J = 8.4 Hz)), 2.43 (t (J = 9.1 Hz), NCH_3 (chelate)); $^{31}P\{^1H\}$ NMR (**10a**) (acetone-d_6) $\delta(P_1)$ 216.7, $\delta(P_2)$ 184.8, $\delta(P_3)$ 173.0 (J_{12} = 10, J_{13} = 67.3, J_{23} = 8 Hz); (**10c**) ($CDCl_3$) $\delta(P_1)$ 219.8, $\delta(P_2)$ 210.2, $\delta(P_3)$ 176.8, $\delta(P_4)$ 183.8, $\delta(P_5)$ 174.4 (J_{12} = 36.8, J_{14} = 6.2, J_{15} = 68.0, J_{23} = 63.7, J_{45} = 6.1 Hz).

***cis*-[Cr(CO)$_2$(CH$_3$N(POCH$_2$CH$_2$O)$_2$)$_2$] (11).** This was identified spectroscopically in the filtrate from the previous reaction; ^1H NMR ($CDCl_3$) δ 2.44 (t (J = 9.0 Hz), NCH_3); $^{31}P\{^1H\}$ NMR ($CDCl_3$) AA'XX', $\delta(P_A)$ 187.8, $\delta(P_X)$ 178.7 (J_{AX} = 59.1 Hz).

***mer*-[W$_2$(CO)$_6$(CH$_3$N(P(OCH$_3$)$_2$)$_2$)$_2$(μ-CH$_3$N(P(OCH$_3$)$_2$)$_2$)] (12).** A toluene solution (15 mL) of 0.30 g (0.833 mmol) of [W(CO)$_3$(CHT)] and 0.269 g (1.25 mmol) of $CH_3N(P(OCH_3)_2)_2$ was stirred at room temperature for 6 h, by which time it was light yellow. The solution was concentrated in vacuo and chromatographed on a 1.5 × 20 cm column of Brockman I alumina. The column was developed with hexane and eluted with 4:1 hexane/diethyl ether, which removed a small yellow band (see results). Further elution with 1:1 hexane/diethyl ether removed a large yellow band, which was taken to dryness and recrystallized from toluene/hexane to give pale yellow crystals (yield 40%). The composition and stereochemistry were obtained from an X-ray crystal structure determination; IR (toluene solution) 1978 (m), 1882 (vs), 1874 (sh), cm^{-1} ($\nu_{C\equiv O}$); ^1H NMR (C_6D_6) δ 3.73 (d (J = 12.2 Hz)), 3.52 (d (J = 13.9 Hz)), 3.47 (d (J = 13.3 Hz), 36 H, OCH_3), 2.99 (t (J = 10.6 Hz), 3 H, NCH_3 (bridge)), 2.35 (t (J = 9.0 Hz), 6 H, NCH_3 (chelate)); $^{31}P\{^1H\}$ NMR (C_6D_6) $\delta(P_1)$ 165.4, $\delta(P_2)$ 128.8, $\delta(P_3)$ 120.0 (J_{12} = 150.8, J_{13} = 41.6, J_{23} = 82.0, $J_{11'}$ = 15.8, $^1J_{W\text{-}P_1}$ = 452.8, $^1J_{W\text{-}P_2}$ = 345.6, $^1J_{W\text{-}P_3}$ = 294.0 Hz).

***mer*-[W(CO)$_3$(CH$_3$N(P(OCH$_3$)$_2$)$_2$)$_2$] (13).** A toluene solution (10 mL) of 0.30 g (0.83 mmol) of [W(CO)$_3$(CHT)] and 0.38 g (1.800 mmol) of $CH_3N(P(OCH_3)_2)_2$ was stirred at room temperature for 1.5 h, by which time the color was bright yellow. A ^{31}P NMR spectrum of the crude mixture indicated incomplete reaction, so the reaction was continued at 60 °C for 6 h and then at room temperature overnight. Solvent was removed in vacuo from the dull gold-colored solution, and the residual oil taken up in 2 mL of toluene and chromatographed on a 1.5 × 20 cm column of Brockman I alumina. The column was developed with hexane and eluted successively with 20-mL portions of hexane/toluene in 9:1, 4:1, and 1:1 ratios, by which time a broad, pale yellow band was evident. Further elution with hexane/diethyl ether (4:1) removed the band, which was collected in two approximately equal fractions. The second fraction was shown by ^{31}P NMR to contain only **12**. Removal of solvent from the first fraction in vacuo followed by two crystallizations from diethyl ether/hexane precipitated more **12**, and from the mother liquor from the second crystallization the desired complex was obtained as a medium yellow oil in low yield following removal of the solvent in vacuo; IR (hexane solution) 1984 (m), 1893 (sh), 1882 (vs) cm^{-1} ($\nu_{C\equiv O}$); ^1H NMR (C_6D_6) δ 3.54–3.42 (m, 24 H, OCH_3), 2.80 (dd (J = 2.4, 9.0 Hz), 3 H, NCH_3 (η^1 ligand)), 2.33 (t (J = 9.0 Hz), 3 H, NCH_3 (η^2 ligand)); $^{31}P\{^1H\}$ NMR (C_6D_6) $\delta(P_1)$ 159.6 (ddd), $\delta(P_2)$ 128.3 (ddd), $\delta(P_3)$ 119.5 (ddd), $\delta(P_4)$ 147.9 (ddd) (J_{12} = 143.2, J_{13} = 40.2, J_{14} = 122.8, J_{23} = 83.5, J_{24} = 4.0, J_{34} = 18.0, $^1J_{W\text{-}P_1}$ = 439.8, $^1J_{W\text{-}P_2}$ = 343.0, $^1J_{W\text{-}P_3}$ = 295.6 Hz).

***cis*-[W(CO)$_4$(CH$_3$N(P(OCH$_3$)$_2$)$_2$)] (14).** A solution of 0.30 g (0.773 mmol) of [W(CO)$_4$(NBD)] and 0.166 g (0.773 mmol) of $CH_3N(P(OCH_3)_2)_2$ in 10 mL of methylcyclohexane was heated at 60 °C for 7 h. The solvent was removed in vacuo at 25 °C, and the resulting oil held under dynamic vacuum for 2 h. Dissolution of the oil in 2 mL of diethyl ether followed by dilution with hexane and slow concentration under reduced pressure afforded the product as white crystals. The mother liquor was removed via syringe, and the crystals were washed with 2 × 2 mL of cold hexane and dried in vacuo (yield 80%). Anal. Calcd for $C_9H_{15}O_8P_2NW$: C, 21.15; H, 2.96. Found: C, 21.6; H, 3.1. IR (toluene solution) 2028 (m), 1933 (m), 1910 (vs) cm^{-1} ($\nu_{C\equiv O}$); ^1H NMR (C_6D_6) δ 3.21 ("virtual" triplet ("J" = 14.0 Hz), 12 H, OCH_3), 2.20 (t (J = 9.1 Hz), 3 H, NCH_3); $^{31}P\{^1H\}$ NMR (C_6D_6) δ(P) 121.6 (s) ($^1J_{W\text{-}P}$ = 306.2 Hz).

***mer*-[W$_2$(CO)$_6$(CH$_3$N(P(OCH(CH$_3$)$_2$)$_2$)$_2$)$_2$(μ-CH$_3$N(P(OCH(CH$_3$)$_2$)$_2$)$_2$)] (17).** A diethyl ether solution (20 mL) of 0.25 g (0.694 mmol) of [W(CO)$_3$(CHT)] and 0.455 g (1.389 mmol) of $CH_3N(P(OCH(CH_3)_2)_2)_2$ was stirred overnight. Solvent was removed from the resulting yellow solution in vacuo, and the residual oil was taken up in hexane and chromatographed on a 1.5 × 20 cm column of Brockman III alumina. Development with hexane removed a small yellow band, which appeared to decompose when the solvent was removed. Elution with 9:1 hexane/diethyl ether removed a large yellow band, leaving an orange–yellow band at the top of the column that could not be eluted. Removal of the

solvent from the second band gave a yellow oil from which a small quantity of pale yellow crystals precipitated over a period of several weeks. The residual oil (vide infra) was transferred to a clean flask via a syringe, and the crystals were washed quickly with cold hexane (in which they were partially soluble) and dried in vacuo. From the ^{31}P NMR spectrum of the crystals, it was evident that they were still contaminated with the oil from which they precipitated, and because of their significant solubility in hexane, further purification was not attempted. The nature of the product is well-established by the spectroscopic data, however; ^1H NMR (C_6D_6) δ 5.25 (m), 4.80 (m, OC*H*(CH_3)$_2$), 1.61–1.18 (m, OCH(CH_3)$_2$), 3.58 (t (J = 15.3 Hz), NCH_3 (bridge)), 2.51 (t (J = 8.8 Hz), NCH_3 (chelate)); $^{31}P\{^1H\}$ NMR (C_6D_6) $\delta(P_1)$ 163.4, $\delta(P_2)$ 119.3, $\delta(P_3)$ 107.1 (J_{12} = 154.7, J_{13} = 39.6, J_{23} = 93.8, $J_{11'}$ = 39.1, $^1J_{W\text{-}P_1}$ = 429.2, $^1J_{W\text{-}P_2}$ = 341.1, $^1J_{W\text{-}P_3}$ = 295.3 Hz).

***mer*-[W(CO)$_3$(CH$_3$N(P(OCH(CH$_3$)$_2$)$_2$)$_2$)$_2$] (18).** The yellow oil removed from the crystals of **17** (previous experiment) was shown by ^1H and ^{31}P NMR to consist of this complex and excess ligand. Separation proved impossible, but the nature of the tungsten complex is satisfactorily established by its spectroscopic data and by its use in the formation of a binuclear tungsten–iridium complex (vide infra); IR (hexane solution) 1977 (m), 1880 (vs), 1870 (vs) cm^{-1} ($\nu_{C\equiv O}$); ^1H NMR (C_6D_6) δ 4.96 (m), 4.70 (m), 4.23 (m) (8 H, OC*H*(CH_3)$_2$), 1.53–1.03 (m, 48 H, OCH(C*H*$_3$)$_2$), 2.96 (dd (J = 2.6, 11.8 Hz), 3 H, NCH_3 (η^1 ligand)), 2.46 (t (J = 8.9 Hz), 3 H, NCH_3 (η^2 ligand)); $^{31}P\{^1H\}$ NMR (C_6D_6) $\delta(P_1)$ 155.5 (ddd), $\delta(P_2)$ 119.9 (dd), $\delta(P_3)$ 110.6 (ddd), $\delta(P_4)$ 137.7 (dd) (J_{12} = 149.8, J_{13} = 39.8, J_{14} = 29.8, J_{23} = 90.0, J_{34} = 1.9, $^1J_{W\text{-}P_1}$ = 432.6, $^1J_{W\text{-}P_2}$ = 336.9, $^1J_{W\text{-}P_3}$ = 297.2 Hz).

Reaction of [W(CO)$_2$(CHT)] with CH$_3$N(POCH$_2$CH$_2$O)$_2$. To a toluene solution (20 mL) of 0.581 g (1.446 mmol) of [W(CO)$_3$(CHT)] was added 0.458 g (2.170 mmol) of solid CH$_3$N(POCH$_2$CH$_2$O)$_2$. After this was stirred for 4 h, a cloudy yellow solution resulted. This was filtered, the solvent removed in vacuo, and the solid washed with two 10-mL portions of hexane and dried in vacuo. The ^{31}P NMR spectrum of this crude solid indicated the presence of *fac*-[W$_2$(CO)$_6$(CH$_3$N(POCH$_2$CH$_2$O)$_2$)$_2$(μ-CH$_3$N(POCH$_2$CH$_2$O)$_2$)] (**19b**) and its fac–mer isomer (**19c**) as the major components. Unfortunately, all attempts at purification led only to ill-defined solids; $^{31}P\{^1H\}$ NMR (acetone/acetone-d_6) (**19b**) $\delta(P_1)$ 156.9, $\delta(P_2)$ 126.5 (J_{12} = 37.2, $J_{11'}$ = 26.6, $J_{22'}$ = 66.3, $^1J_{W\text{-}P_2}$ = 316.7 Hz); (**19c**) $\delta(P_1)$ 168.2 (ddd), $\delta(P_2)$ 156.9 (td), $\delta(P_3)$ 126.5 (d), $\delta(P_4)$ 128.2 (dd), $\delta(P_5)$ 122.3 (dd) (J_{12} = 25.7, J_{14} = 164.9, J_{15} = 41.0, J_{23} = 39.0, J_{45} = 79.2, $^1J_{W\text{-}P_3}$ = 316.7 Hz).

[RhMo(CO)$_4$Cl(CH$_3$N(P(OCH(CH$_3$)$_2$)$_2$)$_2$)$_2$] (20). A solution of 0.257 g (0.518 mmol) of [RhCl(COD)]$_2$ in 10 mL of diethyl ether was treated with carbon monoxide for 10 min and added dropwise to a diethyl ether solution (10 mL) containing 0.866 g (1.037 mmol) of *mer*-[Mo(CO)$_3$(CH$_3$N(P(OCH(CH$_3$)$_2$)$_2$)$_2$)$_2$]. The solution immediately became bright red as carbon monoxide was evolved. After stirring briefly under reduced pressure, the reaction was allowed to proceed at room temperature for 2 h, after which hexane was added and the solution slowly concentrated under reduced pressure. The air-stable, orange crystals that formed were filtered off, washed with a small portion of cold hexane, and dried in vacuo (yield 83%). The ^{31}P NMR spectrum of the product indicated the presence of two isomers. Anal. Calcd for $C_{30}H_{62}O_{12}P_4N_2ClMoRh$: C, 35.99; H, 6.25; Cl, 3.54. Found: C, 36.0; H, 6.4; Cl, 3.8. IR (hexane solution) 1993 (sh), 1985 (m), 1941 (vs), 1878 (s), 1798 (sh) cm^{-1} ($\nu_{C\equiv O}$); $^{31}P\{^1H\}$ NMR (toluene/acetone-d_6, 228 K) (**20a**), AA′MXX′, $\delta(P_A)$ 133.0, $\delta(P_X)$ 165.2 ($J_{P_A\text{-}P_{A'}}$ = 400 (fixed), $J_{P_A\text{-}P_X}$ = 149.5, $J_{P_A\text{-}P_{X'}}$ = 27.5, $J_{P_X\text{-}P_{X'}}$ = 157.6, $^1J_{Rh\text{-}P_A}$ = 141.2 Hz); (**20b**) AA′MXX′ $\delta(P_A)$ 121.9, $\delta(P_X)$ 162.5 ($J_{P_A\text{-}P_{A'}}$ = 454.0, $J_{P_A\text{-}P_X}$ = 208.3, $J_{P_A\text{-}P_{X'}}$ = 45.0, $J_{P_X\text{-}P_{X'}}$ = 135.8, $J_{Rh\text{-}P_A}$ = 144.0 Hz).

[IrMo(CO)$_4$Cl(CH$_3$N(P(OCH(CH$_3$)$_2$)$_2$)$_2$)$_2$] (21). To a solution of *mer*-[Mo(CO)$_3$(CH$_3$N(P(OCH(CH$_3$)$_2$)$_2$)$_2$)$_2$], prepared in situ from 0.30 g (1.103 mmol) of [Mo(CO)$_3$(CHT)] and 0.722 g (2.206 mmol) of CH$_3$N(P(OCH(CH$_3$)$_2$)$_2$)$_2$ in 10 mL of diethyl ether was added 0.370 g (0.551 mmol) of solid [IrCl(COD)]$_2$. Over 0.5 h the solution slowly became brownish yellow, but not all of the [IrCl(COD)]$_2$ had dissolved. Carbon monoxide was then bubbled through the mixture for 5 min, 6 mL of toluene was added to dissolve the residual solid, and the solution was stirred under CO for another 2 h. Removal of solvent from the resulting red–orange solution in vacuo followed by trituration with diethyl ether yielded orange crystals and a dark, red–orange solution. The crystals were filtered off, and the filtrate was diluted with hexane to form a small amount of a gummy solid. The liquid was transferred to a clean flask via syringe and diluted with acetonitrile to form a second crop of orange crystals. The two crops of crystals were combined, washed with cold hexane, and dried in vacuo (yield 73%). Anal. Calcd for $C_{30}H_{62}O_{12}P_4N_2ClMoIr$: C, 33.04; H, 5.74; Cl, 3.52. Found: C, 32.9; H, 5.7; Cl, 3.6. IR (Nujol mull) 1960 (sh), 1951 (s), 1926 (vs), 1868 (vs), 1774 (s) cm^{-1}; (hexane solution) 1958 (m), 1932 (vs), 1880 (s), 1788 (m) cm^{-1} ($\nu_{C\equiv O}$); ^1H NMR ($CDCl_3$) δ 4.87 (sep (J = 5.7 Hz), 4 H), 4.65 (sep (J = 5.4 Hz), 4 H, OC*H*(CH_3)$_2$), 2.59 (t (J = 2.5 Hz), 6 H, NCH_3), 1.39–1.17 (m, 48 H, OCH(C*H*$_3$)$_2$); $^{31}P\{^1H\}$ NMR ($CDCl_3$) AA′XX′, $\delta(P_A)$ 94.7, $\delta(P_X)$ 158.2 ($J_{P_A\text{-}P_{A'}}$ = 402.0, $J_{P_A\text{-}P_X}$ = 155.7, $J_{P_A\text{-}P_{X'}}$ = 26.3, $J_{P_X\text{-}P_{X'}}$ = 170.9 Hz).

[IrW(CO)$_4$Cl(CH$_3$N(P(OCH(CH$_3$)$_2$)$_2$)$_2$)$_2$] (22). To the mixture of *mer*-[W(CO)$_3$(CH$_3$N(P(OCH(CH$_3$)$_2$)$_2$)$_2$)$_2$] and free CH$_3$N(P(OCH(CH$_3$)$_2$)$_2$)$_2$ obtained in the reaction forming **17** (0.673 g total mass; amount of the tungsten complex estimated from the ^{31}P NMR spectrum of the mixture) in 10 mL of toluene was added 0.244 g (0.364 mmol) of solid [IrCl(COD)]$_2$. Carbon monoxide was bubbled through the mixture for 10 min to give a dark brown–red solution, which was stirred under carbon monoxide overnight. The resulting dark orange solution was filtered, and the solvent removed in vacuo. The residue was extracted with 15 mL of hexane, taken up in 10 mL of diethyl ether, and filtered to remove a small quantity of yellow solid. Dilution with hexane and cooling overnight at −5 °C precipitated a gummy green solid. The orange supernatant was transferred to a clean flask via syringe and evaporated to dryness to yield a dark orange solid. Anal. Calcd for $C_{30}H_{62}O_{12}P_4N_2ClWIr$: C, 30.58; H, 5.31; Cl, 3.01. Found: C, 30.4; H, 5.3; Cl, 3.2. Ir (Nujol mull) 1980 (s), 1923 (vs), 1866 (vs), 1767 (s) cm^{-1}; (toluene solution) 1925 (vs), 1871 (m), 1777 (m) cm^{-1} ($\nu_{C\equiv O}$); ^1H NMR (C_6D_6) δ 5.16 (m, 4 H), 4.98 (m, 4 H, OC*H*(CH_3)$_2$), 2.77 (br, 6 H, NCH_3), 1.60–1.14 (m, 48 H, OCH(C*H*$_3$)$_2$); $^{31}P\{^1H\}$ NMR (C_6D_6) AA′XX′, $\delta(P_A)$ 101.9, $\delta(P_X)$ 140.8 ($J_{P_A\text{-}P_{A'}}$ = 403.4, $J_{P_A\text{-}P_X}$ = 155.7, $J_{P_A\text{-}P_{X'}}$, 27.7, $J_{P_X\text{-}P_{X'}}$ = 171.4, $^1J_{W\text{-}P_X}$ = 410.3 Hz).

***fac*-[Mo(CO)$_3$(((C$_6$H$_5$)$_2$P)$_2$CHC$_5$H$_4$N)] (23).** To a solution of 0.50 g (1.84 mmol) of [Mo(CO)$_3$(CHT)] in 30 mL of toluene was added 1.698 g (3.68 mmol) of solid ((C$_6$H$_5$)$_2$P)$_2$CHC$_5$H$_4$N. After 2 h the solution was red–orange, and a golden yellow microcrystalline precipitate had formed. The solid was filtered off and washed with 3 mL of toluene and 5 mL of hexane. Dilution of the filtrate with hexane afforded a second crop of crystals. The solids were combined and recrystallized from acetone/diethyl ether/hexane (yield 85%). Anal. Calcd for $C_{32}H_{25}P_2O_3NMo$: C, 61.06, H, 4.01; N, 2.22. Found: C, 61.3; H, 4.1; N, 2.1. IR (Nujol mull) 1909 (s), 1811 (s), 1804 (s) cm^{-1}; (acetone solution) 1923 (s), 1828 (s), 1814 (s) cm^{-1} ($\nu_{C\equiv O}$); $^{31}P\{^1H\}$ NMR (acetone-d_6) δ 46.4 (s).

***fac*-[W(CO)$_3$(((C$_6$H$_5$)$_2$P)$_2$CHC$_5$H$_4$N)] (24).** This was prepared in an analogous fashion to the previous complex. The orange crystals that precipitated as the reaction proceeded were not particularly soluble, but with difficulty the analytical sample was recrystallized from dichloromethane/diethyl ether, yield 86%. Anal. Calcd for $C_{32}H_{25}P_2O_3NW$: C, 53.57; H, 3.52. Found: C, 52.3; H, 3.5. IR (Nujol mull) 1901 (s), 1799 (vs), 1793 (vs) cm^{-1} ($\nu_{C\equiv O}$); $^{31}P\{^1H\}$ NMR (acetone-d_6) δ 39.1 (s) ($^1J_{W\text{-}P}$ = 179.6 Hz).

***cis*-[Mo(CO)$_4$(((C$_6$H$_5$)$_2$P)$_2$CHC$_5$H$_4$N)] (25).** Carbon monoxide was bubbled through an acetone solution of **23** for 3 h. The solution was diluted with hexane and cooled overnight to precipitate pale yellow needles. The supernatant and some finely divided solid were removed via syringe, and the crystals washed with acetone/diethyl ether and dried in vacuo. The product was identified spectroscopically: IR (acetone solution) 2021 (s), 1936 (s), 1908 (vs), 1897 (vs) cm^{-1} ($\nu_{C\equiv O}$); $^{31}P\{^1H\}$ NMR (acetone-d_6) δ 22.3 (s).

***cis*-[W(CO)$_4$(((C$_6$H$_5$)$_2$P)$_2$CHC$_5$H$_4$N)] (26).** A solution of **24** in toluene was refluxed overnight while carbon monoxide was slowly bubbled through. The solution was concentrated in vacuo and diluted with hexane to afford the product as dull yellow microcrystals in 62% yield. The complex was characterized

Table I. Crystallographic Data for Complexes

	12	16	20	21	27
formula	$C_{21}H_{45}O_{18}P_6N_3W_2$	$C_{17}H_{36}O_{14}P_5N_3W_2$	$C_{30}N_{62}O_{12}P_4N_2ClMoRh$	$C_{30}H_{62}O_12P_4N_2ClMoIr$	$C_{10}H_{20}O_4P_2NClRu$
FW	1181.21	1029.11	1001.12	1090.43	416.77
cryst syst	monoclinic	orthorhombic	orthorhombic	orthorhombic	monoclinic
space group	$P2_1/c$ (No. 14)	$P2_12_12_1$ (No. 19)	$Pna2_1$ (No. 33)	$Pna2_1$ (No. 33)	$P2_1/n$
a, Å	17.421 (3)	14.512 (3)	16.561 (4)	16.545 (3)	7.6964 (8)
b, Å	15.581 (5)	15.202 (4)	12.964 (2)	12.921 (2)	8.8437 (6)
c, Å	17.116 (6)	15.577 (3)	1.530 (5)	21.595 (5)	23.8778 (23)
β, deg	117.26 (2)				96.856 (8)
V, Å^3	4130	3436	4623	4616	1614
Z,	4	4	4	4	4
ρ(calcd), g cm^{-3}	1.90	1.87	1.44	1.57	1.72
radiatn	Mo Kα, graphite monochromated, λ = 0.71073 Å				
linear abs coeff, cm^{-1}	58.9	70.7	8.6	33.8	13.2
range trans factor	0.553–0.999				0.939–0.999
θ range, deg	0.5–24.0	0.5–23.0	1.5–25.0	0.5–25.0	1.5–26.0
scan type	ω–2θ	ω–2θ	ω–2θ	ω–2θ	ω–2θ
scan width, deg	0.80 + 0.20 tan θ	0.80 + 0.20 tan θ	0.80 + 0.20 tan θ	0.80 + 0.20 tan θ	0.80 + 0.20 tan θ
scan rate, deg min^{-1}	1.6–16.5	0.8–4.1	1.3–16.5	1.3–16.5	1.3–16.5
attn factor	11.87	11.87	11.87	11.87	11.87
programs used	Enraf-Nonius SDP	Enraf-Nonius SDP	Enraf-Nonius SDP	Enraf-Nonius SDP	Enraf-Nonius SDP
p factor in weight[e]	0.04	0.04	0.04	0.04	0.04
unique data	6055	2688	4180	4180	2916
data, $I \geq 3.0\sigma(I)$	4282	2233	2685[d]	2923	2791
no. of variables	451	388	359	369	172
largest shift–esd in final cycle	0.12	0.16	0.06	0.11	0.15
R[a]	0.035	0.031	0.045	0.040	0.026
R_w[b,e]	0.044	0.037	0.054	0.053	0.039
GOF[c]	1.36	1.53	1.70	2.19	2.19

[a] $R = \sum||F_o| - |F_c||/\sum|F_o|$. [b] $R_w = [\sum w(|F_o - F_c|)^2/\sum w(F_o)^2]^{1/2}$. [c] GOF = $[\sum w(|F_o - F_c|)^2/(N_o - N_v)]^{1/2}$, where N_o and N_v are, respectively, the number of observations and variables. [d] Data with $I \geq 2.0\sigma(I)$. [e] The weighting scheme used in the final refinement was $w = 1/(\sigma_F)^2$ where $\sigma_F = \sigma_F^2/2F$ and $\sigma_F^2 = [(\sigma_I)^2 + (pF^2)^2]^{1/2}$.

spectroscopically: IR (acetone solution) 2014 (m), 1940 (w), 1898 (vs), 1849 (s) cm^{-1} ($\nu_{C\equiv O}$); $^{31}P\{^1H\}$ NMR (acetone-d_6) δ 34.5 ($^1J_{W-P}$ = 239.6 Hz).

[(η^5-C_5H_5)RuCl($CH_3N(P(OCH_3)_2)_2$)] (27). Dropwise addition of a solution of [CpRu(COD)Cl] (0.166 g, 0.563 mmol) in acetone (5 mL) to 0.231 g (1.072 mmol) of $CH_3N(P(OCH_3)_2)_2$ in 5 mL of acetone produced a dirty yellow–orange solution, which was stirred at room temperature for 36 h. Dilution of the reaction solution with hexane and cooling produced a small amount of an ill-defined precipitate. The mixture was then filtered through a 10 × 2 cm column of Brockman III alumina, and a yellow band could be eluted with acetone. Removal of the acetone in vacuo followed by trituration of the residual oil with hexane containing a few drops of diethyl ether afforded the product as fluffy orange crystals in ca. 60% yield. The air-sensitive complex was characterized by ^1H and ^{31}P NMR spectroscopy, and confirmation was provided by an X-ray structure determination (see Results); ^1H NMR (C_6D_6) δ 4.73 (t (J = 0.9 Hz), 5 H, C_5H_5), 3.93 ("virtual triplet", 6 H, OCH_3), 3.14 ("virtual triplet", 6 H, OCH_3), 2.42 (t (J = 10.4 Hz), 3 H, NCH_3) $^{31}P\{^1H\}$ NMR (C_6D_6) δ(P) 123.4 (s).

[$Rh(CH_3N(P(OCH(CH_3)_2)_2)_2)_2$]$ClO_4$ (28). In acetone 0.251 g (1.21 mmol) of silver perchlorate was reacted with 0.30 g (0.606 mmol) of $[RhCl(COD)]_2$, and the precipitated silver chloride removed by filtration. Addition of 0.793 g (2.42 mmol) of $CH_3N(P(OCH(CH_3)_2)_2)_2$ formed a bright yellow solution, which was concentrated in vacuo and diluted with diethyl ether and hexane. Further concentration in vacuo afforded the product as bright yellow, air-sensitive crystals, which were filtered off, washed with diethyl ether, and dried in vacuo (yield 60%). Anal. Calcd for $C_{26}H_{62}O_{12}N_2ClRh$: C, 36.43; H, 7.30; N, 3.27. Found: C, 35.9; H, 7.2; N, 3.4. ^1H NMR (acetone-d_6) δ 4.84 (m, 8 H, $OCH(CH_3)_2$), 2.66 (q (J = 5.0 Hz), 6 H, NCH_3), 1.42 (t (J = 6.0 Hz), 48 H, $CH(CH_3)_2$); $^{31}P\{^1H\}$ NMR (acetone-d_6) δ 108.0 (d (J_{Rh-P} = 181.8 Hz)).

X-ray Crystallography. All data were collected on an Enraf-Nonius CAD-4 diffractometer at room temperature. General procedures for data collection, reduction, and refinement have been published.[13] Specifics for the present work are listed in Table I. All crystals were mounted on glass fibers and coated with a thin layer of epoxy except for **12**, which was mounted in a nitrogen-filled capillary.

A pale yellow crystal of **12** was grown by slow diffusion of hexane into a toluene solution of the complex. Cell constants were determined by least-squares refinement of the setting angles of 25 reflections (8.0° ≤ θ ≤ 11.8°) that had been accurately centered on the diffractometer. The space group was uniquely determined from the systematic absences observed in the data collection. The intensity monitors showed an approximately linear decrease in intensity of 8.4%, after which a precipitous drop occurred and the crystal appeared black. No better success was had with two other crystals despite great care in excluding air from the capillary mount, so the portion of the data collected prior to the rapid decomposition was retained and corrected for the decay, even though it did not constitute a full hemisphere. An empirical absorption correction employing ψ scans on five reflections with 79° ≤ χ ≤ 83°, collected prior to the rapid decomposition, was applied. Equivalent reflections were averaged resulting in an agreement factor of 0.02 (on F_o). The solution and refinement of the structure proceeded uneventually, and following anisotropic refinement of all non-hydrogen atoms, most hydrogen atoms could be located in a difference map. These were included in idealized positions riding on the attached carbon atoms with isotropic thermal parameters equal to 1.3 times those of the attached carbon atoms. A final difference map showed small residual features (<±1.0 e/Å^3) mainly associated with the tungsten atoms. These are probably due to inadequacies in the absorption correction and/or the effects of crystal decomposition. Final positional parameters are given in Table II, while pertinent metrical parameters appear in Table III. Additional crystallographic data are included as supplementary material (Tables S1–S7; see the paragraph at the end of the paper).

Bright yellow, approximately tetrahedral crystals of **16** were obtained in low yield together with a substantial quantity of **12** in an attempt to grow crystals from one preparation of the latter by slow diffusion of hexane into a toluene solution of the tungsten complexes. Twenty-five reflections with 8.0° ≤ θ ≤ 13.4° were used to determine the cell constants while the space group was uniquely determined by the systematic absences observed in the data collection. A linear decrease of 10.9% in the intensity of the monitor reflections was noted over the course of the data collection, and a correction was made. No absorption correction was made because of the inaccessibility of satisfactory reflections

Table II. Positional Parameters (Esd) for $[W_2(CO)_6(CH_3N(P(OCH_3)_2)_2)_2(\mu\text{-}CH_3N(P(OCH_3)_2)_2)]$[a] (12)

atom	x	y	z	B, Å²
W1	0.16623 (2)	0.22584 (2)	0.34378 (2)	2.730 (7)
W2	−0.26554 (2)	0.21682 (2)	0.25827 (2)	2.948 (8)
P1	0.2990 (1)	0.1891 (2)	0.3406 (2)	4.11 (6)
P2	0.2639 (2)	0.1335 (1)	0.4642 (2)	3.62 (6)
P3	0.0452 (1)	0.2420 (2)	0.3767 (1)	3.26 (5)
P4	0.1397 (1)	0.2182 (1)	0.2332 (1)	3.02 (5)
P5	−0.3512 (2)	0.1033 (2)	0.1567 (2)	4.20 (6)
P6	−0.4061 (2)	0.1939 (2)	0.2462 (2)	4.58 (6)
O4	0.1029 (5)	0.3488 (4)	0.1818 (4)	6.2 (2)
O5	0.0623 (4)	0.0783 (4)	0.2101 (4)	5.0 (2)
O6	0.2379 (5)	0.3960 (4)	0.4550 (5)	6.6 (2)
O7	−0.1595 (4)	0.0992 (4)	0.4230 (4)	5.7 (2)
O8	−0.2203 (5)	0.3719 (5)	0.3871 (5)	7.5 (2)
O9	−0.3552 (4)	0.3497 (5)	0.1043 (4)	6.8 (2)
O11	0.3761 (4)	0.2520 (5)	0.3533 (5)	6.3 (2)
O12	0.3080 (5)	0.1388 (5)	0.2637 (5)	8.1 (2)
O21	0.3171 (5)	0.1637 (5)	0.5637 (5)	7.1 (2)
O22	0.2502 (4)	0.0359 (3)	0.4885 (4)	4.4 (2)
O31	0.0687 (4)	0.3102 (5)	0.4531 (4)	5.3 (2)
O32	0.0074 (4)	0.1646 (4)	0.4088 (4)	6.0 (2)
O41	−0.0895 (4)	0.1334 (4)	0.2337 (4)	4.8 (2)
O42	−0.1650 (3)	0.2565 (4)	0.1370 (3)	3.9 (1)
O51	−0.3345 (4)	0.0015 (4)	0.1641 (5)	5.8 (2)
O52	−0.3911 (4)	0.1104 (5)	0.0518 (5)	5.9 (2)
O61	−0.4317 (5)	0.1646 (7)	0.3199 (5)	9.9 (3)
O62	−0.4840 (4)	0.2613 (5)	0.1980 (5)	6.5 (2)
N1	0.3384 (4)	0.1255 (5)	0.4289 (5)	4.8 (2)
N2	−0.0504 (4)	0.2773 (4)	0.2985 (4)	3.5 (2)
N3	−0.4379 (5)	0.1155 (5)	0.1722 (6)	5.2 (2)
C1	0.4232 (7)	0.0788 (7)	0.4730 (8)	7.2 (4)
C2	−0.0577 (6)	0.3704 (5)	0.2816 (6)	4.6 (3)
C3	−0.5209 (7)	0.0703 (9)	0.1285 (9)	7.9 (4)
C4	0.1228 (5)	0.3028 (5)	0.2401 (6)	3.8 (2)
C5	0.1005 (5)	0.1286 (5)	0.2604 (6)	3.8 (2)
C6	0.2154 (5)	0.3319 (6)	0.4176 (6)	3.9 (2)
C7	−0.1992 (5)	0.1404 (6)	0.3623 (6)	4.0 (2)
C8	−0.2349 (6)	0.3146 (6)	0.3394 (6)	4.6 (3)
C9	−0.3220 (5)	0.2998 (6)	0.1582 (6)	4.2 (2)
C11	0.4192 (8)	0.2996 (8)	0.429 (1)	8.6 (5)
C12	0.272 (1)	0.077 (1)	0.217 (1)	18.1 (7)
C21	0.2879 (9)	0.2180 (8)	0.6065 (8)	7.7 (4)
C22	0.2079 (7)	−0.0226 (6)	0.4174 (7)	5.7 (3)
C31	0.0129 (7)	0.325 (1)	0.4933 (7)	8.4 (4)
C32	0.0531 (6)	0.0980 (7)	0.4628 (7)	6.9 (3)
C41	−0.1162 (6)	0.0485 (6)	0.2264 (8)	7.0 (4)
C42	−0.1059 (6)	0.2498 (8)	0.1002 (6)	5.6 (3)
C51	−0.3082 (8)	−0.0405 (7)	0.2448 (9)	7.7 (4)
C52	−0.3352 (8)	0.1143 (8)	0.0116 (7)	7.3 (4)
C61	−0.3825 (9)	0.134 (1)	0.3969 (8)	11.0 (5)
C62	−0.4807 (8)	0.3416 (9)	0.2364 (9)	8.7 (4)

[a] Anisotropically refined atoms are given in the form of the isotropic equivalent displacement parameter defined as $^4/_3[a^2B(1,1) + b^2B(2,2) + c^2B(3,3) + ab(\cos\gamma)B(1,2) + ac(\cos\beta)B(1,3) + bc(\cos\alpha)B(2,3)]$.

near $\chi = 90°$. The contributions of the hydrogen atoms to the overall scattering were treated as outlined for **12** although not all could be located in difference maps. Following convergence with the original choice of enantiomer, refinement was continued using the other enantiomer, resulting in significantly higher values of R and R_w. The original choice was therefore retained. At the end of the refinement the difference map showed residual features ranging from 1.1 to −1.3 e/Å³, most of which were closely associated with the tungsten atoms and are probably the result of the lack of an absorption correction. Final positional parameters are given in Table IV, while pertinent metrical parameters appear in Table V. Additional crystallographic data are included as supplementary material (Tables S8–S14).

Dark red-orange crystals of **20** were grown by the slow evaporation of a hexane/diethyl ether solution of the complex by using a slow nitrogen purge. Twenty-five reflections having $8.2° \leq \theta \leq 14.8°$ were used to determine the unit cell while the space group was uniquely determined by the systematic absences observed during the data collection. Because of the low linear absorption coefficient, no absorption correction was applied, and the intensity monitors showed only a statistical fluctuation over the course of the data collection. As the refinement proceeded, it became evident that disorder existed between the chlorine atom and the terminal carbonyl group (C(6)O(6)) on rhodium. This was apparent primarily from the significant distortion of the RhC(6)O(6) moiety from linearity, the unusually small thermal parameter for C(6) as compared with those of the other terminal carbonyl groups, and an inability to refine C(6) anisotropically. Also the thermal ellipsoid for the chlorine atom appeared somewhat larger than would be expected for such an atom in a bridging position. We interpret this disorder as the result of the presence in the crystal of two isomeric molecules, the major isomer having the chlorine bridging and a terminal carbonyl group on rhodium, and the minor isomer having the chlorine in a terminal site on rhodium and a second bridging carbonyl group. Such an interpretation is consistent with the observation of two bridging carbonyl bands in the solid-state infrared spectrum and of two isomers by low-temperature ^{31}P NMR spectroscopy. Attempts to model the disorder using partial occupancies of the two sites by both chlorine and carbonyl moieties constrained to reasonable geometries based on the isomeric composition determined from the ^{31}P NMR spectrum as well as by difference Fourier syntheses were unsuccessful. The refinement was therefore completed with chlorine alone assigned to the bridging site and a carbonyl group to the terminal site with C(6) being refined isotropically. This is clearly not entirely satisfactory, as the metrical parameters associated with the disordered atoms are not very meaningful but is unlikely to seriously affect the remainder of the molecules. Many, but not all, of the hydrogen atoms were located at this point and included in idealized positions as described above. Following convergence, refinement of the opposite enantiomer was carried out. This converged at essentially the same values of R and R_w, so the original choice was retained. A final difference map showed features ranging from 0.75 to −0.4/ e/Å³. Final positional parameters are given in Table VI, while Tables VIII and IX present

Table III. Selected Bond Distances (Å) and Interbond Angles (deg) for $[W_2(CO)_6(CH_3N(P(OCH_3)_2)_2)_2(\mu\text{-}CH_3N(P(OCH_3)_2)_2)]$ (12)

Bond Distances

W(1)–P(1)	2.407 (2)	P(1)–N(1)	1.670 (8)
W(1)–P(2)	2.450 (2)	P(2)–N(1)	1.669 (7)
W(1)–P(3)	2.433 (2)	P(3)–N(2)	1.680 (7)
W(2)–P(4)	2.420 (2)	P(4)–N(2)	1.710 (6)
W(2)–P(5)	2.450 (2)	P(5)–N(3)	1.661 (8)
W(2)–P(6)	2.389 (2)	P(6)–N(3)	1.662 (8)
W(1)–C(4)	1.982 (9)	C(4)–O(4)	1.146 (9)
W(1)–C(5)	2.036 (9)	C(5)–O(5)	1.13 (1)
W(1)–C(6)	2.017 (9)	C(6)–O(6)	1.15 (1)
W(2)–C(7)	2.009 (9)	C(7)–O(7)	1.15 (1)
W(2)–C(8)	1.964 (9)	C(8)–O(8)	1.16 (1)
W(2)–C(9)	2.007 (9)	C(9)–O(9)	1.14 (1)

Interbond Angles

P(1)–W(1)–P(2)	64.88 (8)	P(5)–W(2)–C(9)	87.6 (3)
P(1)–W(1)–P(3)	166.82 (8)	P(6)–W(2)–C(7)	97.9 (2)
P(1)–W(1)–C(4)	95.8 (2)	P(6)–W(2)–C(8)	96.5 (3)
P(1)–W(1)–C(5)	92.6 (2)	P(6)–W(2)–C(9)	86.6 (2)
P(1)–W(1)–C(6)	94.2 (2)	C(7)–W(2)–C(8)	88.5 (4)
P(2)–W(1)–P(3)	101.95 (7)	C(7)–W(2)–C(9)	174.8 (3)
P(2)–W(1)–C(4)	160.4 (2)	C(8)–W(2)–C(9)	88.4 (4)
P(2)–W(1)–C(5)	96.0 (2)	W(1)–P(1)–N(1)	97.0 (2)
P(2)–W(1)–C(6)	91.3 (2)	W(1)–P(2)–N(1)	95.4 (3)
P(3)–W(1)–C(4)	97.4 (2)	W(1)–P(3)–N(2)	119.8 (2)
P(3)–W(1)–C(5)	88.3 (2)	W(2)–P(4)–N(2)	121.0 (2)
P(3)–W(1)–C(6)	86.3 (2)	W(2)–P(5)–N(3)	96.1 (3)
C(4)–W(1)–C(5)	87.8 (3)	W(2)–P(6)–N(3)	98.4 (3)
C(4)–W(1)–C(6)	86.8 (3)	P(1)–N(1)–P(2)	102.6 (4)
C(5)–W(1)–C(6)	171.7 (3)	P(3)–N(2)–P(4)	128.1 (3)
P(4)–W(2)–P(5)	100.76 (7)	P(5)–N(3)–P(6)	101.3 (4)
P(4)–W(2)–P(6)	164.28 (9)	W(1)–C(4)–O(4)	175.7 (7)
P(4)–W(2)–C(7)	87.9 (2)	W(1)–C(5)–O(5)	175.7 (7)
P(4)–W(2)–C(8)	98.3 (3)	W(1)–C(6)–O(6)	174.6 (8)
P(4)–W(2)–C(9)	88.4 (2)	W(2)–C(7)–O(7)	177.6 (8)
P(5)–W(2)–P(6)	64.16 (9)	W(2)–C(8)–O(8)	177.9 (9)
P(5)–W(2)–C(7)	96.7 (3)	W(2)–C(7)–O(9)	176.3 (8)
P(5)–W(2)–C(8)	160.4 (3)		

Table IV. Positional Parameters (Esd) for $[W_2(CO)_6(CH_3N(P(OMe)_2)_2)(CH_3OP(N(CH_3)P(OCH_3)_2)_2)]$[a] (16)

atom	x	y	z	B, Å²
W1	0.24009 (4)	0.18405 (3)	0.33035 (4)	2.79 (1)
W2	0.31213 (4)	0.29272 (3)	0.16389 (4)	2.83 (1)
P1	0.3166 (3)	0.0752 (3)	0.4174 (3)	5.1 (1)
P2	0.1768 (4)	0.1565 (4)	0.4732 (3)	6.4 (1)
P3	0.1311 (3)	0.3024 (3)	0.2951 (2)	3.00 (7)
P4	0.2656 (3)	0.4234 (3)	0.2457 (3)	3.62 (8)
P5	0.1535 (3)	0.2723 (3)	0.1194 (2)	3.32 (8)
O1	0.0989 (8)	0.0526 (7)	0.2454 (8)	6.2 (3)
O2	0.3896 (8)	0.0917 (7)	0.2168 (7)	5.4 (3)
O3	0.3765 (9)	0.3178 (9)	0.4263 (7)	7.3 (3)
O4	0.3693 (9)	0.1573 (8)	0.0229 (7)	6.7 (3)
O5	0.3672 (9)	0.4257 (9)	0.0227 (8)	7.6 (3)
O6	0.5171 (8)	0.295 (1)	0.2276 (9)	8.3 (4)
O11	0.345 (2)	−0.0181 (9)	0.3981 (9)	12.9 (6)
O12	0.415 (1)	0.098 (1)	0.464 (1)	9.8 (5)
O21	0.090 (1)	0.134 (1)	0.511 (1)	13.2 (5)
O22	0.191 (1)	0.243 (1)	0.5455 (8)	10.8 (5)
O31	0.0429 (6)	0.3153 (7)	0.3571 (6)	4.1 (2)
O41	0.3334 (7)	0.4666 (7)	0.3169 (8)	5.2 (3)
O42	0.2449 (9)	0.5139 (7)	0.1938 (7)	5.4 (3)
O51	0.1076 (8)	0.3313 (7)	0.0463 (7)	4.7 (2)
O52	0.1328 (7)	0.1748 (7)	0.0856 (6)	4.0 (2)
N1	0.252 (1)	0.0783 (9)	0.5037 (8)	5.3 (3)
N2	0.0765 (8)	0.2942 (8)	0.1982 (7)	3.4 (3)
N3	0.1717 (8)	0.4060 (8)	0.3031 (7)	3.7 (3)
C1	0.150 (1)	0.100 (1)	0.277 (1)	4.0 (3)
C2	0.335 (1)	0.1405 (9)	0.2460 (9)	3.3 (3)
C3	0.325 (1)	0.270 (1)	0.3895 (9)	5.5 (4)
C4	0.346 (1)	0.205 (1)	0.0756 (9)	4.2 (3)
C5	0.347 (1)	0.376 (1)	0.077 (1)	5.0 (4)
C6	0.441 (1)	0.298 (1)	0.205 (1)	4.8 (4)
C7	0.262 (2)	0.032 (1)	0.585 (1)	6.4 (5)
C8	−0.011 (1)	0.342 (1)	0.180 (1)	5.8 (4)
C9	0.124 (1)	0.478 (1)	0.349 (1)	6.8 (5)
C11	0.286 (1)	−0.073 (1)	0.346 (1)	8.8 (6)
C12	0.j.k (1)	0.107 (2)	0.424 (1)	9.0 (7)
C21	0.047 (1)	0.051 (1)	0.482 (2)	11.5 (7)
C22	0.180 (2)	0.242 (2)	0.628 (1)	11.1 (8)
C31	−0.023 (1)	0.247 (1)	0.367 (1)	4.8 (4)
C41	0.423 (1)	0.498 (1)	0.288 (1)	7.8 (6)
C42	0.185 (1)	0.525 (1)	0.127 (1)	6.8 (5)
C51	0.145 (1)	0.328 (1)	−0.0421 (9)	6.8 (5)
C52	0.040 (1)	0.146 (1)	0.060 (1)	5.2 (4)

[a] Anisotropically refined atoms are given in the form of the isotropic equivalent displacement parameter defined as $^4/_3[a^2B(1,1) + b^2B(2,2) + c^2B(3,3) + ab(\cos\gamma)B(1,2) + ac(\cos\beta)B(1,3) + bc(\cos\alpha)B(2,3)]$

pertinent bond distances and interbond angles. Additional crystallographic data are given as supplementary material (Table S15–S21).

Orange crystals of **21**, were obtained by the slow evaporation of a solution of the complex in hexane/diethyl ether by using a nitrogen purge. The near identity of the unit cell dimensions, determined from 25 reflections with $8.0 \leq \theta \leq 11.9$, with those for **20** strongly suggested that the two are isomorphous. This was confirmed by the systematic absences observed in the data collection. A linear correction was applied to compensate for a 4.3% decline in the intensities of the monitor reflections, but no absorption correction was made because of the inaccessibility of suitable reflections near $\chi = 90°$. The structure was solved by direct methods and refined uneventfully. Those hydrogen atoms that could be located in difference maps were treated as described above. Following convergence of the original model, the other enantioner was refined, which gave significantly higher values for R and R_w, so the original choice was retained. Final positional parameters are given in Table VII, while Tables VIII and IX give pertinent bond distance and interbond angles. Other crystallographic data are given as supplementary material (Tables S22–S28).

A dark orange crystal of **27**, obtained from the slow evaporation of a diethyl ether solution of the complex under nitrogen, was cleaved to give a sample of suitable size. Twenty-five reflection

Table V. Selected Bond Distances (Å) and Interbond Angles (deg) for $[W_2(CO)_6(CH_3N(P(OCH_3)_2)_2)(CH_3OP(N(CH_3)P(OCH_3)_2)_2)]$ (16)

Bond Distances			
W(1)–P(1)	2.412 (4)	P(1)–N(1)	1.64 (1)
W(1)–P(2)	2.443 (4)	P(2)–N(1)	1.68 (1)
W(1)–P(3)	2.459 (4)	P(3)–N(2)	1.71 (1)
W(2)–P(4)	2.457 (4)	P(3)–N(3)	1.69 (1)
W(2)–P(5)	2.424 (4)	P(4)–N(3)	1.65 (1)
W(1)–C(1)	2.01 (2)	P(5)–N(2)	1.69 (1)
W(1)–C(2)	2.01 (1)	C(1)–O(1)	1.14 (2)
W(1)–C(3)	2.02 (2)	C(2)–O(2)	1.18 (2)
W(2)–C(2)	2.67 (1)	C(3)–O(3)	1.19 (2)
W(2)–C(4)	1.98 (1)	C(4)–O(4)	1.15 (2)
W(2)–C(5)	1.92 (2)	C(5)–O(5)	1.18 (2)
W(2)–C(6)	1.97 (2)	C(6)–O(6)	1.17 (2)

Interbond Angles			
P(1)–W(1)–P(2)	62.8 (2)	C(2)–W(2)–C(5)	151.3 (6)
P(1)–W(1)–P(3)	157.6 (1)	C(2)–W(2)–C(6)	76.3 (6)
P(1)–W(1)–C(1)	95.4 (4)	C(4)–W(2)–C(5)	83.5 (6)
P(1)–W(1)–C(2)	80.0 (4)	C(4)–W(2)–C(6)	90.8 (7)
P(1)–W(1)–C(3)	84.9 (4)	C(5)–W(2)–C(6)	87.2 (7)
P(2)–W(1)–P(3)	95.0 (2)	W(1)–C(2)–W(2)	86.7 (5)
P(2)–W(1)–C(1)	91.3 (4)	W(1)–P(1)–N(1)	100.1 (5)
P(2)–W(1)–C(2)	142.6 (4)	W(1)–P(2)–N(1)	97.8 (5)
P(2)–W(1)–C(3)	85.7 (4)	W(1)–P(3)–N(2)	116.2 (4)
P(3)–W(1)–C(1)	87.5 (4)	W(1)–P(3)–N(3)	116.3 (4)
P(3)–W(1)–C(2)	122.3 (4)	W(2)–P(4)–N(3)	112.2 (4)
P(3)–W(1)–C(3)	90.9 (5)	W(2)–P(5)–N(2)	113.2 (4)
C(1)–W(1)–C(2)	88.0 (6)	N(2)–P(3)–N(3)	107.1 (6)
C(1)–W(1)–C(3)	176.5 (7)	P(1)–N(1)–P(2)	99.3 (7)
C(2)–W(1)–C(3)	95.5 (7)	P(3)–N(2)–P(5)	110.4 (6)
P(4)–W(2)–P(5)	89.5 (1)	P(3)–N(3)–P(4)	113.5 (7)
P(4)–W(2)–C(4)	167.1 (5)	W(1)–C(1)–O(1)	179 (1)
P(4)–W(2)–C(5)	84.5 (5)	W(1)–C(2)–O(2)	157 (1)
P(4)–W(2)–C(6)	93.4 (6)	W(1)–C(3)–O(3)	177 (1)
P(5)–W(2)–C(4)	87.4 (5)	W(2)–C(4)–O(4)	177 (1)
P(5)–W(2)–C(5)	97.8 (6)	W(2)–C(5)–O(5)	178 (2)
P(5)–(W2)–C(6)	174.5 (6)	W(2)–C(6)–O(6)	175 (2)
C(2)–W(2)–C(4)	73.6 (6)		

with $21.8° \leq \theta \leq 25.8°$ were used to determine the unit cell, and the systematic absences observed during the data collection uniquely determined the space group. Only statistical fluctuations were noted in the intensities of the monitor reflections, and ψ scans on six reflections having $81° \leq \chi \leq 88°$ were used to determine an empirical absorption correction. Equivalent reflections were averaged with an agreement factor (on F_o) of 0.018. The refinement proceeded uneventfully. Hydrogen atoms were included in calculated positions and treated as described above. The final difference map was essentially featureless. Final positional parameters are given in Table X, while pertinent bond distances and interbond angles appear in Table XI. All other crystallographic data are given as supplementary material (Tables S29–S35).

Results

Synthesis of Complexes. Reaction of $[M(CO)_3(CHT)]$ (M = Cr, Mo, W) with the ligands $CH_3N(P(OR)_2)_2$ (general symbol PNP; specific symbols L_2 (R = CH_3), L_2' (R = $CH(CH_3)_2$), L_2'' (R = CH_2–)) using a ligand:metal ratio of 1.5:1 yields as the primary product complexes of composition $[M_2(CO)_6(PNP)_2(\mu\text{-PNP})]$. In those instances where pure materials could be obtained, these formed colorless to pale yellow air-sensitive crystals. In solvents in which the products are appreciably soluble (e.g., toluene or diethyl ether) and particularly under forcing conditions these have been identified from their infrared and ^{31}P NMR spectra as having the meridional configuration about both metals. Thus the ^{31}P NMR spectra show three multiplet resonances of equal intensity, which are assigned respectively to P_1, P_2, and P_3 in order of increasing field. These assignments and the determination of the coordination geometry derive from the observation in the Mo and W

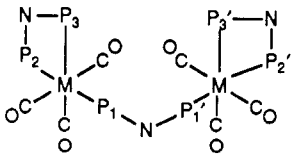

1a, Mo, L_2
2, Mo, L_2'
5, Cr, L_2
7, Cr, L_2'
10a, Cr, L_2''
12, W, L_2
17, W, L_2'

complexes of one large (J_{12}) and two smaller (J_{13} and J_{23}) phosphorus–phosphorus coupling constants which indicate a trans disposition[30] of P_1 and P_2 with P_3 situated cis to both. Confirmation was obtained from a structure determination of **12**. The assignments for the Cr complexes were made by analogy, which requires that J_{12} be smaller than J_{13} and J_{23}. This is consistent with earlier results that indicate that in related Cr(0) complexes, $^2J_{P-P}$(trans) is generally less than $^2J_{P-P}$(cis).[30] With the exception of **7**, whose ^{31}P NMR spectrum is apparently first order, all the complexes in this group exhibit second-order effects in their ^{31}P NMR spectra which are attributable to a nonzero coupling between the two phosphorus atoms of the bridging ligand ($J_{11'}$). This is most apparent in the resonance assigned to P_1, which appears as either a double doublet of nonbinomial triplets (**12**) or as a doublet of multiplets. Weak lines flanking the major doublet of doublet resonances for P_2 and P_3 are also seen, and all spectra could be satisfactorily simulated only when a nonzero value for $J_{11'}$ was used (representative comparison of observed and calculated spectra are included as supplementary material). All complexes that could be isolated as pure compounds showed three carbonyl absorptions characteristic of the *mer*-{$M(CO)_3$} moiety[31] although in most instances the two lower energy bands showed significant overlap.

Under mild reaction conditions and particularly when the products crystallized from solution as formed, the $[M_2(CO)_6(PNP)_2(\mu\text{-PNP})]$ complexes could be obtained as isomeric mixtures. One component has the facial configuration about both metals (**1b**, **4**, **19b**) while the other

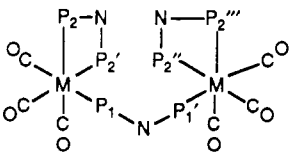

1b, Mo, L_2
4, Mo, L_2''
19b, W, L_2''

has the facial configuration about one metal and the meridional configuration about the other (**1c**, **10c**, **19c**). The

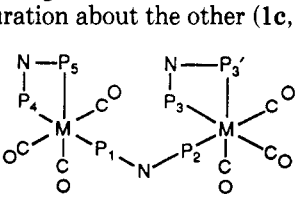

1c, Mo, L_2
10c, Cr, L_2''
19c, W, L_2''

(30) Verkade, J. G. *Coord. Chem. Rev.* **1972/73**, *9*, 1.
(31) King, R. B.; Lee, T. W. *Inorg. Chem.* **1982**, *21*, 319.

Table VI. Positional Parameters (Esd) for $[RhMoCl(CO)_4(MeN(P(OPr^i)_2)_2)_2]$[a] (20)

atom	*x*	*y*	*z*	*B*, Å^2
Rh	0.82194 (5)	0.01694 (6)	0.288	3.66 (1)
Mo	0.79942 (5)	0.00584 (7)	0.15652 (6)	3.48 (2)
P1	0.9195 (2)	0.1428 (2)	0.2804 (2)	3.94 (6)
P2	0.9014 (2)	0.1376 (2)	0.1449 (2)	3.83 (6)
P3	0.7035 (2)	−0.1321 (2)	0.1727 (2)	4.07 (7)
P4	0.7323 (2)	−0.1140 (2)	0.3076 (2)	4.16 (7)
Cl	0.9052 (3)	−0.1015 (3)	0.2197 (2)	7.7 (1)
N1	0.9423 (5)	0.1858 (7)	0.2103 (5)	4.4 (2)*
N2	0.6853 (6)	−0.1649 (7)	0.2474 (5)	4.9 (2)*
C1	1.0055 (8)	0.268 (1)	0.2054 (7)	6.9 (3)
C2	0.6260 (9)	−0.253 (1)	0.2594 (7)	7.4 (4)
C3	0.7195 (7)	0.085 (1)	0.1075 (7)	5.5 (3)
C4	0.7396 (6)	0.0991 (7)	0.2222 (6)	3.4 (2)
C5	0.8252 (7)	−0.046 (1)	0.0726 (6)	5.2 (3)
C6	0.8291 (6)	0.0376 (8)	0.3856 (5)	3.6 (2)*
O3	0.6739 (6)	0.135 (1)	0.0816 (6)	9.9 (3)
O4	0.6951 (4)	0.1600 (6)	0.2375 (4)	5.4 (2)
O5	0.8352 (8)	−0.069 (1)	0.0231 (5)	10.9 (4)
O6	0.8044 (8)	0.071 (1)	0.4150 (7)	11.3 (4)*
O11	1.0075 (4)	0.1106 (6)	0.3022 (4)	5.1 (2)*
O12	0.9079 (4)	0.2448 (6)	0.3214 (4)	4.4 (2)*
O21	0.9802 (4)	0.1148 (6)	0.1027 (4)	4.7 (2)*
O22	0.8780 (5)	0.2471 (6)	0.1159 (4)	5.1 (2)*
O31	0.7167 (5)	−0.2415 (6)	0.1389 (4)	5.1 (2)*
O32	0.6098 (5)	−0.1163 (6)	0.1532 (4)	5.2 (2)*
O41	0.7671 (6)	−0.2150 (8)	0.3359 (5)	8.2 (3)*
O42	0.6609 (4)	−0.0923 (6)	0.3557 (4)	4.7 (2)*
C11	1.0304 (8)	0.089 (1)	0.3680 (7)	5.5 (3)*
C12	0.8308 (8)	0.294 (1)	0.3309 (7)	6.0 (3)*
C21	1.0232 (8)	0.0175 (9)	0.1022 (6)	5.1 (3)*
C22	0.8510 (8)	0.258 (1)	0.0514 (7)	6.1 (3)*
C31	0.7935 (7)	−0.288 (1)	0.1284 (7)	5.4 (3)*
C32	0.5815 (9)	−0.112 (1)	0.0907 (8)	7.1 (4)*
C41	0.815 (1)	−0.236 (1)	0.3818 (9)	9.2 (5)*
C42	0.6168 (9)	0.004 (1)	0.3540 (7)	6.2 (3)*
C111	1.079 (1)	−0.008 (1)	0.3657 (9)	8.5 (5)
C112	1.077 (1)	0.178 (1)	0.391 (1)	15.2 (6)
C121	0.832 (1)	0.342 (1)	0.3953 (9)	8.9 (5)
C122	0.8182 (9)	0.373 (1)	0.280 (1)	8.4 (4)
C211	1.0554 (9)	0.005 (1)	0.353 (8)	8.3 (4)
C212	1.0896 (8)	0.019 (1)	0.1489 (9)	8.2 (4)
C221	0.795 (1)	0.349 (2)	0.053 (1)	11.9 (6)
C222	0.920 (1)	0.278 (1)	0.0088 (8)	8.2 (5)
C311	0.7909 (8)	−0.338 (1)	0.0649 (8)	7.5 (4)
C312	0.8091 (9)	−0.366 (1)	0.1802 (8)	7.8 (4)
C321	0.520 (1)	−0.031 (1)	0.088 (1)	14.3 (9)
C322	0.545 (1)	−0.219 (1)	0.076 (1)	11.4 (6)
C411	0.897 (1)	−0.224 (2)	0.383 (2)	17 (1)
C412	0.783 (2)	−0.340 (2)	0.410 (1)	17.8 (8)
C421	0.547 (1)	−0.005 (1)	0.314 (1)	10.5 (6)
C422	0.595 (1)	0.025 (1)	0.419 (1)	11.4 (6)

[a] Starred atoms were refined isotropically. Anisotropically refined atoms are given in the form of the isotropic equivalent displacement parameter defined as $^4/_3[a^2B(1,1) + b^2B(2,2) + c^2B(3,3) + ab(\cos\gamma)B(1,2) + ac(\cos n\beta)B(1,3) + bc(\cos\alpha)B(2,3)]$.

all-fac isomers are characterized by ^{31}P NMR spectra consisting of two multiplet resonances of relative intensity 2:1, which can be satisfactorily simulated as AA′A″A‴XX′ spin systems (P_1 = X, P_2 = A). The one complex of this group obtained as a single isomer (**4**) exhibited two carbonyl absorptions characteristic of a *fac*-{$M(CO)_3$} moiety.[32] The fac-mer isomers were identified from their ^{31}P NMR spectra, which consist of five first-order multiplets having relative intensities of 1:1:2:1:1 and assigned to P_1–P_5, respectively. As before, the presence of one large coupling constant (J_{14}) in **1c** and **19c** indicates a trans disposition of P_1 and P_4, but the presence of a resonance of intensity 2 (P_3) which has only relatively small couplings to it indicates a mutually cis disposition of three phosphorus

(32) King, R. B.; Raghuveer, K. S. *Inorg. Chem.* **1984**, *23*, 2482.

Table VII. Positional Parameters (Esd) for $[IrMo(CO)_4Cl(MeN(P(OP^i)_2)_2)_2]$[a] (21)

atom	x	y	z	B, Å²
Ir	0.67444 (3)	0.01734 (4)	0.178	3.474 (8)
Mo	0.69580 (7)	0.00605 (9)	0.31048 (6)	2.92 (2)
Cl	0.5926 (2)	−0.0987 (3)	0.2490 (2)	4.64 (9)
P1	0.7646 (2)	−0.1166 (3)	0.1620 (2)	4.02 (9)
P2	0.7929 (2)	−0.1306 (3)	0.2969 (2)	3.93 (9)
P3	0.5943 (2)	0.1382 (3)	0.3229 (2)	3.88 (9)
P4	0.5763 (2)	0.1442 (3)	0.1872 (2)	2.97 (8)
O3	0.6672 (8)	−0.062 (1)	0.4465 (8)	9.0 (4)
O4	0.8014 (7)	0.160 (1)	0.2316 (6)	6.2 (3)
O5	0.8248 (8)	0.146 (1)	0.3775 (7)	8.3 (4)
O6	0.6957 (8)	0.071 (1)	0.0469 (5)	7.1 (3)
O11	0.8333 (6)	−0.095 (1)	0.1144 (5)	5.0 (2)*
O12	0.7306 (7)	−0.2190 (9)	0.1343 (6)	5.7 (3)*
O21	0.8847 (6)	−0.1153 (8)	0.3163 (5)	5.2 (2)*
O22	0.7799 (6)	−0.2406 (8)	0.3327 (5)	4.9 (2)*
O31	0.6151 (7)	0.2493 (9)	0.3525 (5)	5.1 (2)*
O32	0.5160 (6)	0.1161 (8)	0.3646 (5)	4.4 (2)*
O41	0.5902 (6)	0.2454 (8)	0.1465 (5)	4.7 (2)*
O42	0.4867 (6)	0.1130 (8)	0.1640 (5)	4.8 (2)*
N1	0.8120 (7)	−0.170 (1)	0.2213 (6)	4.8 (3)*
N2	0.5504 (7)	0.1872 (9)	0.2584 (6)	4.1 (3)*
C2	0.489 (1)	0.268 (1)	0.2620 (9)	7.0 (5)
C1	0.871 (1)	−0.255 (1)	0.2108 (9)	6.6 (5)
C3	0.679 (1)	−0.037 (1)	0.3977 (7)	5.1 (4)
C4	0.7562 (7)	0.1001 (9)	0.2417 (7)	3.1 (3)
C5	0.7758 (9)	0.091 (1)	0.3555 (8)	4.8 (4)
C6	0.6880 (9)	0.053 (1)	0.0984 (9)	5.0 (4)
C11	0.881 (1)	0.002 (1)	0.1163 (9)	6.2 (5)*
C12	0.680 (1)	−0.228 (2)	0.083 (1)	9.0 (6)*
C21	0.911 (1)	−0.113 (2)	0.379 (1)	6.9 (5)*
C22	0.701 (1)	−0.285 (1)	0.3418 (8)	4.7 (3)*
C31	0.646 (1)	0.264 (1)	0.4164 (9)	5.9 (4)*
C32	0.474 (1)	0.016 (1)	0.3670 (9)	5.3 (4)*
C41	0.668 (1)	0.298 (2)	0.141 (1)	6.3 (5)*
C42	0.465 (1)	0.085 (2)	0.1022 (9)	6.0 (4)*
C111	0.915 (2)	0.015 (2)	0.049 (1)	10.3 (7)
C112	0.952 (1)	−0.019 (2)	0.168 (2)	12.3 (9)
C121	0.711 (2)	−0.332 (2)	0.050 (2)	15 (1)
C122	0.593 (1)	−0.225 (2)	0.089 (1)	12.4 (9)
C211	0.950 (1)	−0.207 (2)	0.399 (1)	9.6 (7)
C212	0.976 (1)	−0.021 (2)	0.391 (2)	11.3 (9)
C221	0.701 (1)	−0.329 (2)	0.4048 (9)	8.1 (6)
C222	0.686 (1)	−0.370 (2)	0.292 (1)	8.3 (6)
C311	0.702 (2)	0.359 (2)	0.414 (2)	11.6 (9)
C312	0.580 (1)	0.278 (1)	0.461 (1)	7.2 (5)
C321	0.442 (1)	0.007 (2)	0.434 (1)	8.6 (6)
C322	0.407 (1)	0.022 (2)	0.319 (1)	7.1 (5)
C411	0.667 (1)	0.349 (2)	0.0791 (9)	7.8 (5)
C412	0.678 (1)	0.372 (2)	0.193 (1)	7.5 (6)
C421	0.426 (2)	0.172 (2)	0.072 (1)	13.6 (8)
C422	0.415 (1)	−0.003 (1)	0.106 (1)	9.2 (6)

[a] Starred atoms were refined isotropically. Anisotropically refined atoms are given in the form of the isotropic equivalent displacement parameter defined as $^4/_3[a^2B(1,1) + b^2B(2,2) + c^2B(3,3) + ab(\cos\gamma)B(1,2) + ac(\cos\beta)B(1,3) + bc(\cos\alpha)B(2,3)]$.

atoms (P_2, P_3, $P_{3'}$) on the second metal.

Reaction of $[Mo(CO)_3(CHT)]$ with a 2-fold excess of $CH_3N(P(OCH(CH_3)_2)_2)_2$ affords a yellow–orange air-sensitive oil in good yield following chromatographic purification. This has been identified spectroscopically as *mer*-$[Mo(CO)_3(\eta^2\text{-}L_2')(\eta^1\text{-}L_2')]$ (**3**). Chromium and tungsten analogues with this ligand as well as with $CH_3N(P(OCH_3)_2)_2$ could be identified as minor products (also oils) in similar reactions with $[M(CO)_3(CHT)]$ (M = Cr, W). The major product of these latter reactions was *mer*-$[M_2(CO)_6(PNP)_2(\mu\text{-PNP})]$. The ^{31}P NMR spectra of these complexes show four first-order multiplets of equal intensity, three of which occur at chemical shifts comparable to those seen in the corresponding *mer*-$[M_2(CO)_6(PNP)_2(\mu\text{-PNP})]$ complexes and are accordingly assigned to the three coordinated phosphorus atoms (P_1–P_3). The fourth occurs close to the chemical shift for the free ligand and is therefore assigned to the uncoordinated end of a monodentate ligand (P_4). This assignment is confirmed for **13** by the absence of ^{183}W satellites for this last resonance. The meridional configuration is indicated in **3**, **13**, and **18** by the one large coupling (J_{12}) between two of the three coordinated phosphorus atoms and by the infrared spectra of **3**, **13**, and **18**, which show the characteristic three carbonyl absorptions expected for a *mer*-$\{M(CO)_3\}$ moiety. Unlike the $[M_2(CO)_6(PNP)_2(\mu\text{-PNP})]$ complexes in which the resonances for the *N*-methyl protons appear as apparent triplets, the $[M(CO)_3(\eta^2\text{-PNP})(\eta^1\text{-PNP})]$ complexes exhibit a doublet of doublets for the *N*-methyl protons of the monodentate ligand.

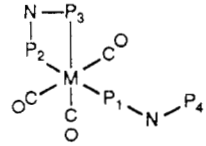

3, Mo, L_2'
6, Cr, L_2
8, Cr, L_2'
13, W, L_2
18, W, L_2'

Table VIII. Selected Bond Distances (Å) for $[MMo(CO)_4Cl(CH_3N(P(OCH(CH_3)_2)_2)_2)_2]$ (Me = Rh, Ir)

	M = Rh (**20**)	M = Ir (**21**)
M–Mo	2.858 (1)	2.888 (1)
M–P(1)	2.302 (3)	2.309 (3)
M–P(4)	2.294 (3)	2.316 (3)
M–Cl	2.533 (4)[a]	2.538 (4)
M–C(4)	2.24 (1)	2.21 (1)
M–C(6)	2.12 (1)[a]	1.79 (2)
Mo–P(2)	2.416 (3)	2.405 (3)
Mo–P(3)	2.417 (3)	2.410 (3)
Mo–Cl	2.618 (5)[a]	2.551 (4)
Mo–C(3)	1.98 (1)	1.98 (1)
Mo–C(4)	2.11 (1)	2.16 (1)
Mo–C(5)	1.97 (1)	1.97 (1)
P(1)–N(1)	1.65 (1)	1.65 (1)
P(2)–N(1)	1.683 (9)	1.74 (1)
P(3)–N(2)	1.69 (1)	1.69 (1)
P(4)–N(2)	1.65 (1)	1.69 (1)
C(3)–O(3)	1.14 (1)	1.12 (2)
C(4)–O(4)	1.13 (1)	1.10 (1)
C(5)–O(5)	1.12 (1)	1.18 (2)
C(6)–O(6)	0.87 (2)[a]	1.14 (2)

[a] Affected by disorder.

As noted in the Experimental Section, the reactions of $[Cr(CO)_3(CHT)]$ with $CH_3N(P(OR)_2)_2$ (R = $CH(CH_3)_2$, CH_2–) produced, in addition to the species described above, minor amounts of species whose ^{31}P NMR spectra could be satisfactorily simulated as AA′XX′ spin systems. These are tentatively formulated as *cis*-$[Cr(CO)_2(PNP)_2]$ (PNP = L_2' (**9**), L_2'' (**11**)). Complex **9** was obtained together with a considerable amount of **8** in the third fraction from chromatographic separation of the crude reaction mixture. The infrared spectrum of this fraction clearly showed weak carbonyl absorptions at 2017 and 1906 cm^{-1} in addition to those assigned to **8**. These are consistent with the presence of a *cis*-$\{Cr(CO)_2\}$ moiety and provide further support for the proposed formulation. The close similarity of the ^{31}P NMR spectrum of **11** to that of **9** suggests an analogous formation, although its poorer quality made identification of the weak outer lines difficult so that a complete simulation was not possible.

The ^{31}P NMR spectra of the crude mixtures obtained from several reactions of $[W(CO)_3(CHT)]$ and $CH_3N(P(OCH_3))_2)_2$ consistently showed resonances for a number of minor products in addition to those assigned to **12** and

Table IX. Interbond Angles (deg) for $[MMo(CO)_4Cl(CH_3N(P(OCH(CH_3)_2)_2)_2)_2]$ (M = Rh, Ir)

	M = Rh (**20**)	M = Ir (**21**)
Mo-M-P(1)	93.29 (9)	91.73 (9)
Mo-M-P(4)	93.46 (8)	92.0 (1)
Mo-M-Cl	57.7 (1)[a]	55.64 (9)
Mo-M-C(4)	46.9 (3)	48.0 (4)
Mo-M-C(6)	173.9 (3)[a]	161.4 (5)
P(1)-M-P(4)	172.6 (1)	174.7 (1)
P(1)-M-Cl	90.4 (1)[a]	89.5 (1)
P(1)-M-C(4)	92.6 (2)	93.4 (3)
P(1)-M-C(6)	86.7 (3)[a]	88.2 (4)
P(4)-M-Cl	90.6 (1[a]	89.5 (1)
P(4)-M-C(4)	94.3 (2)	91.9 (3)
P(4-)-M-C(6)	87.0 (3)[a]	89.4 (4)
Cl-M-C(4)	104.7 (3)[a]	103.6 (4)
Cl-M-C(6)	128.4 (3)[a]	143.0 (5)
C(4)-M-C(6)	127.0 (4)[a]	113.4 (6)
M-Mo-P(2)	88.61 (8)	89.9 (1)
M-Mo-P(3)	88.88 (8)	89.4 (1)
M-Mo-Cl	54.9 (1)[a]	55.21 (9)
M-Mo-C(3)	153.6 (4)	159.8 (5)
M-Mo-C(4)	50.8 (3)	49.3 (3)
M-Mo-C(5)	126.0 (4)	122.8 (4)
P(2)-Mo-P(3)	176.2 (1)	177.7 (1)
P(2)-Mo-Cl	87.8 (1)[a]	89.6 (1)
P(2)-Mo-C(3)	89.6 (3)	89.9 (4)
P(2)-Mo-C(4)	89.6 (2)	91.1 (3)
P(2)-Mo-C(5)	92.51 (3)	91.2 (4)
P(3)-Mo-Cl	88.4 (1)[a]	88.1 (1)
P(3)-Mo-Cl(3	91.4 (3)	90.0 (4)
P(3)-Mo-C(4)	91.1 (2)	90.0 (3)
P(3)-Mo-C(5)	91.3 (3)	91.1 (4)
Cl-Mo-C(3)	98.7 (4)[a]	104.6 (5)
Cl-Mo-C(4)	105.7 (3)[a]	104.5 (3)
Cl-Mo-C(5)	179.0 (4)[a]	177.9 (1)
C(3)-Mo-C(4)	155.5 (5)	150.9 (6)
C(3)-Mo-C(5)	80.4 (5)	77.4 (6)
C(4)-Mo-C(5)	75.2 (5)	73.5 (5)
M-P(1)-N(1)	117.6 (3)	120.4 (4)
Mo-P(2)-N(1)	117.2 (3)	116.9 (4)
Mo-P(3)-N(2)	116.1 (4)	118.2 (4)
M-P(4)-N(2)	117.2 (4)	119.3 (4)
M-Cl-Mo	67.4 (1)[a]	69.15 (9)
P(1)-N(1)-P(2)	123.2 (5)	121. (7)
P(3)-N(2)-P(4)	124.3 (6)	121.1 (6)
Mo-C(3)-O(3)	177 (1)	174.0 (1)
M-C(4)-Mo	82.3 (3)	82.7 (4)
M-C(4)-O(4)	123.1 (9)	129.0 (1)
Mo-C(4)-O(4)	155 (1)	148.0 (1)
Mo-C(5)-O(5)	174 (1)	177.0 (3)
Mo-C(6)-O(6)	139 (1)[a]	177.0 (2)

[a] Affected by disorder.

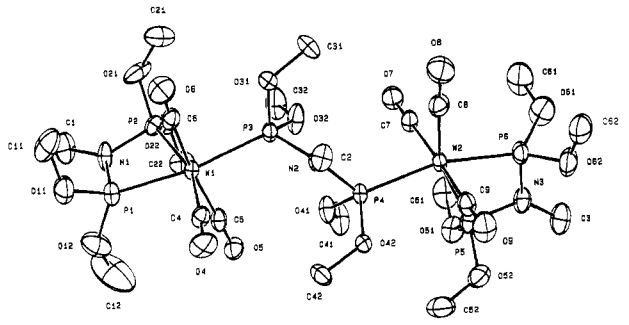

Figure 1. Perspective view of $[W_2(CO)_6(CH_3N(P(OCH_3)_2)_2)_2(\mu\text{-}CH_3N(P(OCH_3)_2)_2)]$ (**12**) with hydrogen atoms omitted for clarity. Thermal ellipsoids are drawn at the 30% probability level.

13. One of these, an upfield singlet with ^{183}W satellites, was tentatively assigned to $[W(CO)_4(L_2)]$ (**14**) and confirmed by an independent synthesis of **14** from $[W(CO)_4(NBD)]$ and 1 equiv of L_2. The yield of **14** varied from run to run but was generally greatest under more strenuous conditions where decomposition of the starting complex and/or intermediate species to furnish the additional carbon monoxide required would be favored. Also found in variable yield was a yellow species, **15**, whose ^{31}P NMR spectrum is a simple AB pattern ($\delta(P_A)$ 126.2, $\delta(P_B)$ 117.4 (J_{AB} = 67.0, $^1J_{W\text{-}P_A}$ = 371.6, $^1J_{W\text{-}P_B}$ = 292.5 Hz (C_6D_6))). This species was the major component of the first fraction obtained in the chromatographic workup of the crude reaction mixture but could never be obtained completely free of **14** (when present) or **12**. Nevertheless, slow diffusion of hexane into a diethyl ether solution containing a mixture of **12** and **15** afforded light yellow, air-sensitive crystals of the latter which were shown by X-ray crystallography to be the novel cycloheptatriene-bridged dimer $[(W(CO)_3(L_2))_2(\mu\text{-}C_7H_8)]$ (**15**). Details of this structure will be published separately. In some runs, a second AB pattern with $\delta(P_A)$ 126.0, $\delta(P_B)$ 116.4 (J_{AB} = 65.8, $^1J_{W\text{-}P_A}$ = 365.0, $^1J_{W\text{-}P_B}$ = 295.7 Hz) was evident. The proximity of these values to those of **15** suggests that this second species is a different conformer or possibly an isomer of **15**.

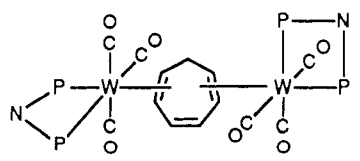

15

In one run of the reaction of $CH_3N(P(OCH_3)_2)_2$ with $[W(CO)_3(CHT)]$ under the conditions described in the Experimental Section, the major chromatographic fraction

Table X. Positional Parameters (Esd) for $[(\eta^5\text{-}C_5H_5)RuCl(CH_3N(P(OCH_3)_2)_2)]$ (27)

atom	*x*	*y*	*z*	*B*, Å^2
Ru	0.12989 (3)	0.19356 (2)	0.81980 (1)	2.236 (4)
Cl	0.44312 (9)	0.1634 (1)	0.82071 (4)	3.93 (2)
P1	0.1387 (1)	0.38226 (8)	0.88256 (3)	2.78 (1)
P2	0.13469 (9)	0.10685 (8)	0.90742 (3)	2.69 (1)
N	0.1391 (4)	0.2745 (3)	0.9405 (1)	3.29 (5)
O1	−0.0270 (3)	0.4886 (3)	0.8862 (1)	4.04 (5)
O2	0.2852 (3)	0.5081 (3)	0.8986 (1)	4.28 (5)
O3	0.2944 (3)	0.0211 (3)	0.9432 (1)	3.94 (5)
O4	−0.0196 (3)	0.0109 (3)	0.9286 (1)	4.40 (5)
C1	−0.0708 (5)	0.6049 (4)	0.8452 (2)	5.02 (8)
C2	0.4669 (5)	0.4692 (5)	0.9086 (2)	5.7 (1)
C3	0.3477 (5)	−0.1226 (5)	0.9254 (2)	5.54 (9)
C4	−0.1953 (5)	0.0678 (6)	0.9190 (2)	6.7 (1)
C5	0.1406 (6)	0.3131 (4)	0.9997 (2)	5.3 (1)
C6	−0.1309 (4)	0.2284 (4)	0.7747 (1)	3.84 (7)
C7	−0.0123 (5)	0.2898 (4)	0.7397 (2)	3.91 (7)
C8	0.0948 (5)	0.1724 (5)	0.7253 (2)	4.63 (8)
C9	0.0398 (5)	0.0352 (4)	0.7491 (2)	5.19 (8)
C10	−0.0996 (4)	0.0725 (4)	0.7792 (1)	4.31 (7)

[a] Anisotropically refined atoms are given in the form of the isotropic equivalent displacement parameter defined as $^4/_3[a^2B(1,1) + b^2B(2,2) + c^2B(3,3) + ab(\cos\gamma)B(1,2) + ac(\cos\beta)B(1,3) + bc(\cos\alpha)B(2,3)]$.

Table XI. Selected Bond Distances (Å) and Interbond Angles (deg) for $[(\eta^5\text{-}C_5H_5)RuCl(CH_3N(P(OCH_3)_2)_2)]$ (27)

Bond Distances			
Ru-Cl	2.4230 (5)	Ru-C(8)	2.248 (2)
Ru-P(1)	2.2384 (5)	Ru-C(9)	2.239 (2)
Ru-P(2)	2.2244 (5)	Ru-C(10)	2.190 (2)
Ru-C(6)	2.183 (2)	P(1)-N	1.679 (2)
Ru-C(7)	2.254 (2)	P(2)-N	1.678 (2)
Interbond Angles			
Cl-Ru-P(1)	97.21 (2)	P(1)-Ru-C′	122.2
Cl-Ru-P(2)	92.80 (2)	P(2)-Ru-C′	122.0
P(1)-Ru-P(2)	68.38 (2)	P(1)-N-P(2)	96.7 (1)
Cl-Ru-C′	133.8[a]		

[a] C′ is the centroid of the cyclopentadienyl ring.

was concentrated, diluted with toluene, and layered with hexane in an attempt to grow crystals of **12**. Accompanying these was a small quantity of bright yellow crystals that were shown from a crystal structure determination to be $[W_2(CO)_6(\eta^2\text{-}CH_3N(P(OCH_3)_2)_2)(\mu\text{-}\eta^3\text{-}CH_3OP(N(CH_3)P(OCH_3)_2)_2)]$ (**16**). Unfortunately there was insufficient material available to obtain satisfactory NMR spectra, and as far as can be determined we have been unable to obtain **16** again despite repeated efforts. There is no indication that the $CH_3N(P(OCH_3)_2)_2$ used contained $CH_3OP(N(CH_3)P(OCH_3)_2)_2$ as an impurity, so we conclude that **16** was formed either during the original reaction or during the chromatographic workup of the crude reaction mixture.

Addition of 0.5 equiv of $[RhCl(CO)_2]_2$, prepared in situ from $[RhCl(COD)]_2$, to **3** readily forms dark red–orange air-stable crystals that analyze as $[RhMoCl(CO)_4(L_2')_2]$ (**20**). An iridium analogue (**21**) could be obtained similarly

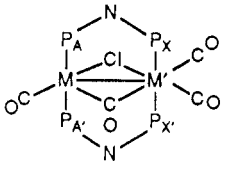

	M	M′	PNP
20a	Rh	Mo	L_2'
21	Ir	Mo	L_2'
22	Ir	W	L_2'

as air-stable orange crystals from **3** and $[IrCl(COD)]_2$ followed by reaction with carbon monoxide, and this latter procedure also served to form the corresponding tungsten–iridium complex (**22**) from the inseparable mixture of **18** and L_2' described earlier. The structures of **20** and **21** have been determined by X-ray crystallography, and that of **22** is assumed to be the same from the close similarity of its ^{31}P NMR and infrared spectra to those for **21**. Thus for **21** and **22** four carbonyl absorptions are seen which are consistent with the observed structure, while the ^{31}P NMR spectra can be satisfactorily simulated as AA′XX′ spin systems. The assignment of the downfield resonance to the phosphorus atoms coordinated to the group VI metal is confirmed by the observation of ^{183}W satellites for this resonance in the spectrum of **22**. The infrared spectrum of **20** in the carbonyl region is more complex than those of **21** and **22**, particularly in the observation of multiple bands in the bridging carbonyl region. Also, its ^{31}P NMR spectrum shows evidence for dynamic behavior. At low temperature a static spectrum is observed that shows two distinct pairs of multiplets which can be simulated as AA′MXX′ (M = Rh) spin systems. Clearly **20** is an isomeric mixture and from the structural study (vide infra) it appears that the major isomer has the structure shown in **20a** while the minor isomer has that shown in **20b**.

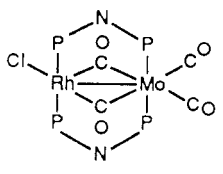

20b

Reaction of a 2-fold excess of $((C_6H_5)_2P)_2CHC_5H_4N$ with $[M(CO)_3(CHT)]$ (M = Mo, W) forms air-stable crystalline products analyzing as $[M(CO)_3(((C_6H_5)_2P)_2CHC_5H_4N)]$ (M = Mo (**23**), W (**24**)). The observation of three carbonyl absorptions indicates a fac arrangement of the carbonyl groups, and the lack of reaction of **23** with excess ligand

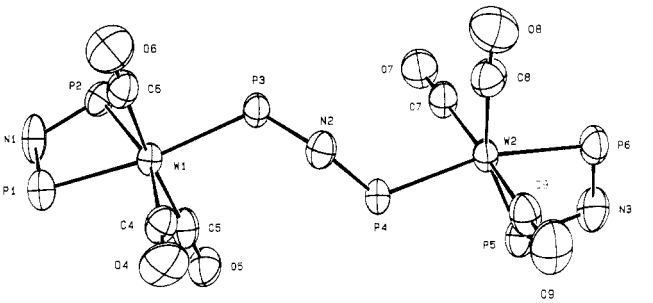

Figure 2. Inner coordination sphere of $[W_2(CO)_6(CH_3N(P(OCH_3)_2)_2)_2(\mu\text{-}CH_3N(P(OCH_3)_2)_2)]$ (**12**). Thermal ellipsoids are drawn at the 50% probability level.

even in boiling toluene indicates that the ligand is coordinated through nitrogen as well as through phosphorus. Slow reaction of **23** and **24** does occur with carbon monoxide however, and the infrared spectra of the products (**25** and **26**) show four bands consistent with the presence of a cis-disubstituted $\{M(CO)_4\}$ moiety.[33] The singlet ^{31}P resonance indicates both phosphorus atoms remain coordinated, so displacement of the pyridyl arm by carbon monoxde evidently has occurred.

Several attempts were made to prepare cyclopentadienylruthenium complexes of $CH_3N(P(OCH_3)_2)_2$ containing either one or two monodentate PNP ligands but without success. Even slow addition of [cpRu(COD)Cl] to an excess of the ligand formed only $[cpRuCl(CH_3N(P(OCH_3)_2)_2)]$ (**27**), while [cpRu(CHT)]PF_6 proved unreactive. With the expectation of synthesizing $[cpRu(\eta^2\text{-}L_2)(\eta^1\text{-}L_2)]^+$, **27** was treated with 1 equiv of silver triflate whereupon a copious precipitate formed. Following addition of 1 equiv of ligand to the filtered solution, several attempts were made to obtain a solid product but to no avail. The ^{31}P NMR spectrum of the resulting reaction mixture indicated considerable **27** remained, although a small quantity of what could be $[cp_2Ru_2(L_2)_2(\mu\text{-}L_2)]^{2+}$ was suggested by this spectrum. Extraction of the orange oil remaining after solvent removal with diethyl ether followed by slow evaporation of the extract formed large orange crystals that were shown to be **27** by a crystal structure study.

Unlike $CH_3N(P(OCH_3)_2)_2$, which reacts with $[Rh(COD)(acetone)_x]ClO_4$ to give the purple dimeric complex $[Rh_2(L_2)_2(\mu\text{-}L_2)_2](ClO_4)_2$,[13] $CH_3N(P(OCH(CH_3)_2)_2)_2$ gives only monomeric $[Rh(L_2')_2]ClO_4$ (**28**) even when the reaction is conducted at −78 °C. The monomeric formulation is indicated by the bright yellow color and by the ^{31}P NMR spectrum, which appears as a simple doublet.

Crystal Structures. The crystal structure of **12** consists of bimetallic $[W_2(CO)_6(L_2)_2(\mu\text{-}L_2)]$ molecules with no unusual intermolecular contacts. A perspective view of the molecule is shown in Figure 1, while Figure 2 presents the inner coordination sphere. The two metal coordination spheres are approximately the same and can be described as distorted octahedral. The distortions can be attributed to the constraints of the chelating ligand and the minimization of intramolecular contacts. Thus the average interligand P–W–P angle of 101.36 (7)° is noticeably larger than the average of the P(1)–W(1)–C(4) and P(4)–W(2)–C(8) angles (97.1 (3)°) since the substituents on P(3) and P(4) are bulkier than the carbonyl groups C(4)O(4) and C(8)O(8). Also, the average of the angles P(3)–W(1)–C(4) and P(4)–W(2)–C(8) (97.8 (3)°) is opened significantly from the ideal 90° value as the result of contacts of these carbonyl groups with methoxy groups on the

(33) Hutchinson, B.; Nakamoto, K. *Inorg. Chem. Acta* **1969**, *3*, 591.

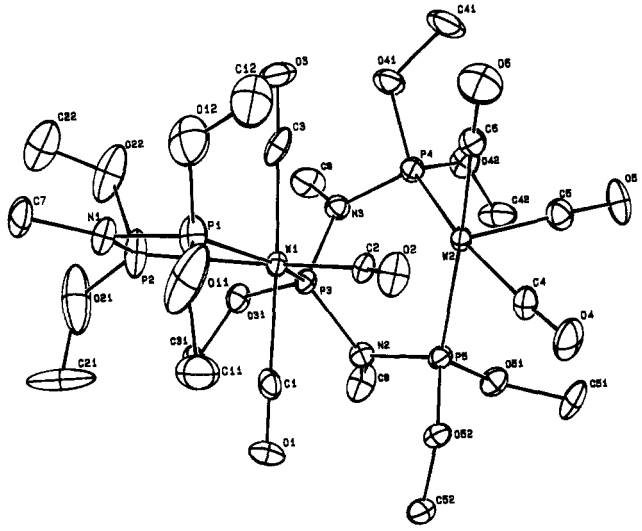

Figure 3. Perspective view of $[W_2(CO)_6(CH_3N(P(OCH_3)_2)_2)(CH_3OP(N(CH_3)P(OCH_3)_2)_2)]$ (**16**) with hydrogen atoms omitted for clarity. Thermal ellipsoids are drawn at the 30% probability level.

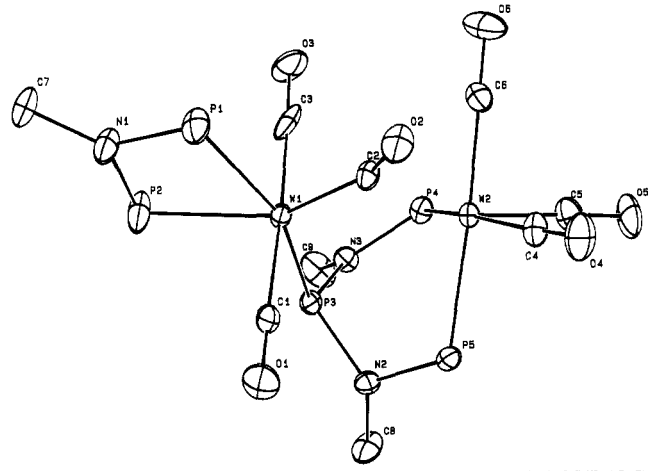

Figure 4. Inner coordination sphere of $[W_2(CO)_6(CH_3N(P(OCH_3)_2)_2)(CH_3OP(N(CH_3)P(OCH_3)_2)_2)]$ (**16**). Thermal ellipsoids are drawn at the 50% probability level.

bridging ligand (O(4)--H(422) = 2.70 Å, O(8)--H(312) = 2.82 Å). The W–P distances vary significantly, although corresponding pairs between each end of the molecule are essentially the same. The range spanned is comparable to W–P distances observed previously in W(0) complexes of trialkyl phosphites (e.g., 2.489 (2) Å in $[W(P(OCH_3)_3)(CO)_2(\mu\text{-}CO)(\mu\text{-}DPPM)(\mu\text{-}C(O)CH_2C_6H_4CH_3)Re(CO)_3]$[34] and 2.415 (5) Å in *mer*-$[W(CO)_3(P(OCH_3)_3)(P(OC_2H_5)_3)(CH_3O_2CC_2CO_2CH_3)]$[35]). The longest distances (W(1)–P(2), W(2)–P(5)) are those trans to the carbonyl groups C(4)O(4) and C(8)O(8), and the distances W(1)–C(4) and W(2)–C(8) are significantly shorter than the other W–C distances, consistent with the expectation that the carbonyl group is a better π-acceptor than is the phosphorus ligand. In each end of the molecule the WP_3 and WC_3 planes are approximately perpendicular while the two WP_3 planes are also approximately perpendicular.

The crystal structure of **16** consists of bimetallic $[W_2(CO)_6(CH_3N(P(OCH_3)_2)_2)(CH_3OP(N(CH_3)P(OCH_3)_2)_2)]$ molecules with no unusual intermolecular contacts. Figures 3 and 4 respectively present perspective views of the entire molecule and the inner coordination sphere. Of particular note are the presence of a $CH_3OP(N(CH_3)P(OCH_3)_2)_2$ ligand and the different coordination about the two metal atoms. The tridentate ligand is structurally analogous to $RP(CH_2PR_2)_2$ (R = CH_3 (dmmm), C_6H_5 (dpmp)), which have been studied extensively by Balch et al. It was found that dpmp coordinates through the terminal phosphorus atoms in *cis*-$[M(CO)_4(dpmp)]$ (M = Cr, Mo, W),[36,37] with the central phosphorus atom then capable of coordinating to a second metal atom to form *trans*-$[Rh(CO)Cl(Mo(CO)_4(dpmp))_2]$ or *cis*-$[PdCl_2(\mu\text{-}dpmp)PdCl_2(CH_3CN)]$. In these complexes the dpmp ligand is in the "extended" conformation so there is no close approach of the metal atoms. The opposite situation occurs in $[Rh_2(\mu\text{-}dmmm)_2(CO)_2]^{2+}$, where the central phosphorus atoms of the two ligands coordinate to one metal and the free ends all coordinate to the second, giving a close metal–metal separation of 2.777 (1) Å.[38] Complex **16** presents an intermediate case wherein the single bridging tridentate ligand adopts the "folded" conformation so that the metal–metal distance is 3.2479 (8) Å. Here again, the terminal phosphorus atoms are coordinated to one metal and the central phosphorus coordinates to the second.

Before discussing the implications of the metal–metal distance, it should be noted that while W(1) is six-coordinate with a meridional arrangement of phosphorus atoms and carbonyl groups quite similar to that in **12**, W(2) possesses only five ligands within normal bonding distances and the three carbonyl groups adopt a facial arrangement. W(2) is thus formally a 16-electron species and appears to remove the electron deficit via interaction with the carbonyl group C(2)O(2) bound to W(1). The primary evidence for the semibridging character of the carbonyl is the W(1)–C(2)–O(2) angle of 157 (1)°; all of the remaining carbonyl groups are essentially linear. Additionally the W(2)–C(2) distance is 2.67 (1) Å. These values are both smaller than those found for the semibridging carbonyl (W–C = 2.97 (3) Å, W–C–O = 172.9 (4)°) in $[(\eta^5\text{-}C_5H_5)_2W_2(CO)_6(\mu\text{-}\eta^2\text{-}C_2H_2)]$[39] and comparable to other carbonyl groups characterized as semibridging.[40] While the semibridging character of C(2)O(2) could well be sufficient to hold the molecule in the observed conformation, it is possible that some degree of metal–metal bonding (W(1)–W(2)) also is present. Thus the W(1)–W(2) distance is only marginally longer than that in $[(\eta^5\text{-}C_5H_5)_2W_2(CO)_6]$ (3.222 (1) Å)[41] and is shorter than that in $[W_2(CO)_6(\mu\text{-guaiazulene})]$ (3.264 (1) Å),[42] both of which necessarily possess a tungsten–tungsten single bond.

The coordination sphere of W(1) is somewhat more distorted from ideal octahedral geometry than are those of the metals in **12**, but apart from the features noted above, the remaining metrical parameters are unexceptional.

Following the observation of disorder in the structure of **20**, the structure of the iridium analogue, **21**, was determined in order to better define the geometry associated

(34) Jeffrey, J. C.; Orpen, A. G.; Stone, F. G. A.; Went, M. J. *J. Chem. Soc., Dalton Trans.* **1986**, 173.
(35) Berke, H.; Huttner, G.; Sontag, C.; Zsolnai, L. *Z. Naturforsch.* **1985**, *40b*, 799.
(36) Balch, A. L.; Guimerans, R. R.; Linehan, J. *Inorg. Chem.* **1985**, *24*, 290.
(37) Guimerans, R. R.; Olmstead, M. M.; Balch, A. L. *Inorg. Chem.* **1983**, *22*, 2224.
(38) Balch, A. L.; Olmstead, M. M.; Oram, D. E. *Inorg. Chem.* **1986**, *25*, 298.
(39) Ginley, D. S.; Bock, C. R.; Wrighton, M. S.; Fischer, B.; Tipton, D. L.; Bau, R. *J. Organomet. Chem.* **1978**, *157*, 41.
(40) Crabtree, R. H.; Lavin, M. *Inorg. Chem.* **1986**, *25*, 805.
(41) Adams, R. D.; Collins, D. M.; Cotton, F. A. *Inorg. Chem.* **1974**, *13*, 1086.
(42) Cotton, F. A.; Hanson, B. E. *Inorg. Chem.* **1976**, *15*, 2806.

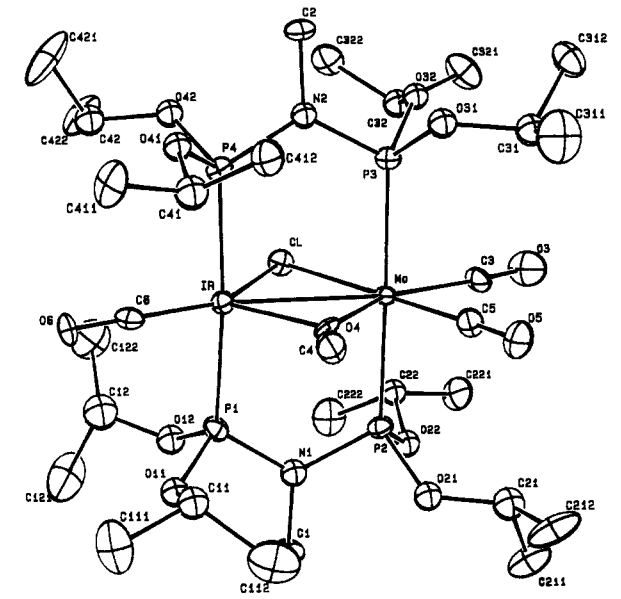

Figure 5. Perspective view of $[IrMo(CO)_4Cl(CH_3N(P(OCH(CH_3)_2)_2)_2)_2]$ (**21**) with hydrogen atoms omitted for clarity. Thermal ellipsoids are drawn at the 30% probability level.

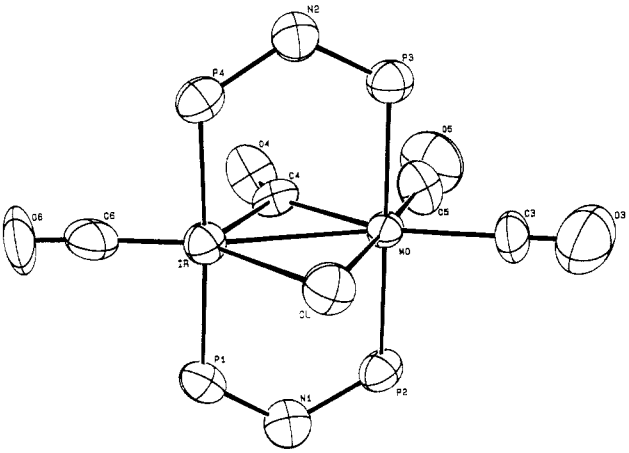

Figure 6. Inner coordination sphere of $[IrMo(CO)_4Cl(CH_3N(P(OCH(CH_3)_2)_2)_2)_2]$ (**21**). Thermal ellipsoids are drawn at the 50% probability level.

with the bridging ligands. The two complexes are essentially isostructural as can be seen from Tables VIII and IX, where the only substantial differences in bond distances and interbond angles between **20** and **21** are those involving chloride and the carbonyl group C(6)O(6). These are the two ligands involved in the disorder in **20**, and there these parameters are not reliable. Figures 5 and 6 depict, respectively, the full molecule and the inner coordination sphere for **21**, while Figure S1 (supplementary material) shows the inner coordination sphere of **20** and the evidence for the disorder. The crystal structures of **20** and **21** consist of discrete heterobimetallic molecules with no unusual intermolecular contacts. From Figure 6 and Table IX the coordination about molybdenum is essentially octahedral, while that about rhodium or iridium is distorted trigonal bipyramidal. Two significant features are the metal–metal distance (2.858 (1) Å (**20**), 2.888 (1) Å (**21**)) and the presence of strongly bridging carbonyl and chloride ligands. While the presence of the latter probably contributes to the close approach of the metals, several features suggest that metal–metal bonding is present. First, the metal–metal distances are considerably shorter than the Rh–Mo distance (3.122 (0) Å) in $[RhMo(CO)_4(C{\equiv}CCH_3)(\mu\text{-}DPPM)_2]$[43] and are significantly shorter than those found in $[(\eta^5\text{-}C_5(CH_3)_5)Rh(\mu\text{-}P(CH_3)_2)_2Mo(CO)_4]$ (2.9212 (7) Å)[44] and $[(\eta^5\text{-}C_5(CH_3)_5)Rh(CH_3)(\mu\text{-}P(CH_3)_2)_2Mo(CO)_2I]$ (2.957 (1) Å),[45] where metal–metal bonding is required to give closed shell configurations to both metals. Further, the Mo–Rh distance is significantly shorter than the intraligand P–P separations (P(1)--P(2) = 2.934 (4), P(3)--(4) = 2.952 (5) Å) which is consistent with an attractive metal–metal interaction. Because of the presence of the bridging chloride and carbonyl ligands it is difficult to decide how to describe this interaction, but a comparison with $[RhMo(CO)_4(C{\equiv}CCH_3)(\mu\text{-}DPPM)_2]$[43] is instructive. There, the Rh–Mo distance is 3.122 (0) Å, and while the propynyl group forms an unsymmetrical, side-on π-bond to molybdenum, there is at best only a slight semibridging character to rhodium in the carbonyl group on the opposite side of the metal–metal axis. Thus the molybdenum(0) center has an 18-electron configuration while the rhodium(I) center is a 16-electron species, consistent with its nearly square-planar coordination. In **21**, the chloride is nearly symmetrically bridging. The Ir–Cl distance of 2.538 (4) Å is much longer than in four-coordinate chlorocarbonyliridium(I) complexes (e.g., 2.405 (3) Å in *trans*-$[Ir(CO)Cl(Bu^t_2P(CH_2)_{10}PBu^t_2)]$[46]) and is still longer than in the chloro-bridged species $[Ir(CF_3C_2CF_3)(C_8H_{12})(\mu\text{-}Cl)]_2$ (2.438 (3), 2.508 (3) Å),[47] $[Ir(\eta^2{:}\eta^3\text{-}C_8H_{11})(C(CF_3)C(CF_3)H)(\mu\text{-}Cl)]^2$ (2.454 (6), 2.480 (6) Å),[48] and $[((C_2H_5)_3P)_2Rh(\mu\text{-}H)_2(\mu\text{-}Cl)IrH_2(P(C_2H_5)_3)_2]$ (2.494 (3) Å).[49] The Mo–Cl distance of 2.551 (4) Å is only slightly longer and is quite comparable to those found in chloro-bridged dimolybdenum species such as $[Mo_2(CO)_4(P(OCH_3)_3)_4(\mu\text{-}Cl)_3][MoOCl_4(OP(OCH_3)_2)]$ (2.533 (6)–2.564 (6) Å)[50] and $[cp_2Mo_2(\mu\text{-}Cl)(\mu\text{-}C_8(CH_3)_8)]SbCl_4$ (2.533 (4), 2.580 (5) Å).[51] In fact it is comparable to or even shorter than a number of terminal Mo–Cl distances such as 2.542 (9) Å in $[cpMo(CO)_3Cl]$[52] and 2.598 (5) Å in $[(\eta^7\text{-}C_7H_7)Mo(CO)_2Cl]$.[53] The carbonyl group C(4)O(4) is nearly symmetrically bridging in **21** and somewhat less so in **20**. The greater degree of asymmetry in the latter complex is mirrored in a more asymmetrically bridging chloride, although the disorder here makes the apparent difference in the metal–chlorine distances less certain. As a consequence of the significant interaction of this carbonyl group with iridium, the coordination geometry departs significantly from square planar. With C(4)O(4) apparently behaving as an almost normal bridging carbonyl group and the chlorine donating a pair of electrons to molybdenum, each metal would then have essentially a 17-electron configuration, and a formal 2-electron Ir–Mo bond is required to account for the observed diamagnetism. This argument is less certain for **20**.

The Mo–P distances in **20** and **21** compare well with

(43) Blagg, A.; Robson, R.; Shaw, B. L.; Thornton-Pett, M. *J. Chem. Soc., Dalton Trans.* **1987**, 2171.
(44) Finke, R. G.; Gaughan, G.; Pierpont, C. G.; Cass, M. E. *J. Am. Chem. Soc.* **1981**, *103*, 1394.
(45) Finke, R. G.; Gaughan, G.; Pierpont, C. G.; Noordik, J. H. *Organometallics* **1983**, *2*, 1481.
(46) March, E. C.; Mason, R.; Thomas, K. M.; Shaw, B. L. *J. Chem. Soc., Chem. Commun.* **1975**, 584.
(47) Clarke, D. A.; Kemmitt, R. D. W.; Russell, D. R.; Tucker, P. A. *J. Organomet. Chem.* **1975**, *93*, C37.
(48) Russell, D. R.; Tucker, P. A. *J. Organomet. Chem.* **1977**, *125*, 303.
(49) Lehner, H.; Musco, A.; Venanzi, L. M.; Albinati, A. *J. Organomet. Chem.* **1981**, *213*, C46.
(50) Drew, M. G. B.; Wilkins, J. D. *J. Chem. Soc., Dalton Trans.* **1975**, 1984.
(51) Bott, S. G.; Connelly, N. G.; Green, M.; Norman, N. C.; Orpen, A. G.; Paxton, J. F.; Schaverien, C. J. *J. Chem. Soc., Chem. Commun.* **1983**, 378.
(52) Chairvosie, S.; Fern, R. H. *Acta Crystallogr.* **1968**, *B24*, 525.
(53) Ziegler, M. L.; Sasse, H. E.; Nuber, B. *Z. Naturforsch.* **1975**, *30b*, 26.

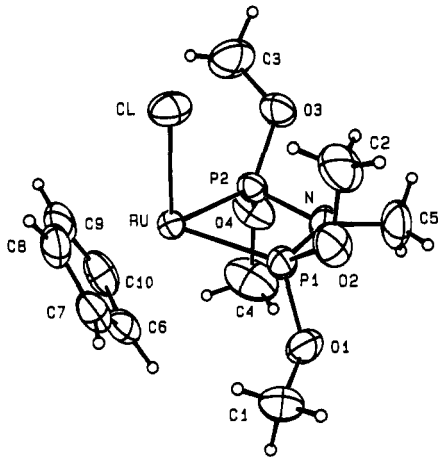

Figure 7. Perspective view of $[(\eta^5\text{-}C_5H_5)RuCl(CH_3N(P(OCH_3)_2)_2)]$ (**27**). Thermal ellipsoids are drawn at the 30% probability level. Hydrogen atoms are drawn artificially small for clarity.

those found previously in $[Mo_2(CO)_4(P(OCH_3)_2)_4(\mu\text{-}Cl)_3][MoOCl_4(OP(OCH_3)_2)]$ (2.402 (6)–2.438 (6) Å)[50] and $[(\eta^3\text{-}C_3H_5)MoCl(CO)_2(P(OCH_3)_3)_2]$ (2.432) (6), 2.425 (6) Å),[54] while the Rh–P and Ir–P distances are only slightly longer than those found[13] in $[Ir(CO)(CH_3N(P(OCH_3)_2)_2)nP(C_6H_5)_3)_2]ClO_4$ and $[Rh_2(CH_3N(P(OCH_3)_2)_2)_2(\mu\text{-}CH_3N(P(OCH_3)_2)_2)_2](CF_3SO_3)_2$. The remaining metrical parameters are unremarkable.

The crystal structure of **27** consists of well-separated $[(\eta^5\text{-}C_5H_5)RuCl(CH_3N(P(OCH_3)_2)_2)]$ molecules. A perspective view is shown in Figure 7. The coordination about ruthenium is quite similar to that observed previously in $[(\eta^5\text{-}C_5H_5)RuClL_2]$ (L = $P(C_6H_5)_3$, $P(CH_3)_3$)[55] and $[(\eta^5\text{-}C_5H_5)Ru(NCC(CN)C(CN)_2)(P(C_6H_5)_3)(P(OCH_3)_3)]$[56] but with some distortion as a result of the four-membered chelate ring. The Ru–P distances differ significantly with the longer distance (Ru–P(1)) associated with a moderate contact between one of the methoxy groups on P(1) and the cyclopentadienyl group (H(13)--H(7) = 2.62 Å). It is tempting to attribute the difference to a lengthening of Ru–P(1) by this contact, but the Ru–$P(OCH_3)_3$ distance (2.239 (2) Å) in $[(\eta^5\text{-}C_5H_5)Ru(NCC(CN)C(CN)C(CN)_2(P(C_6H_5)_3)(P(OCH_3)_3)]$ is essentially the same. Thus with the data available it is not possible to determine whether Ru–P(1) is longer or whether Rh–P(2) is shorter than would be expected. The Ru–Cl distance is slightly shorter than found previously,[55,57,58] while the Ru–C distances are comparable to earlier determinations. As was noted in $[(\eta^5\text{-}C_5H_5)RuCl(P(C_6H_5)_3)(\eta^1\text{-DPPM})]$[58] the Ru–C distances trans to chloride (Ru–C(6) = 2.183 (2) Å; Ru–C(10) = 2.190 (2) Å) are significantly shorter than those trans to phosphorus (2.239 (2)–2.254 (2) Å.) presumably because of differing trans influences of these two ligands.

Discussion

One of the initial goals of this work was the synthesis of *mer*-$[M(CO)_3(\eta^2\text{-PNP})(\eta^1\text{-PNP})]$ (M = Cr, Mo, W) analogues of known DPPM complexes[59,60] used in forming heterobimetallic complexes,[43,59–61] for the synthesis of heterobimetallic complexes in which access to the metal atoms could be varied by changes in the steric bulk of the substituents on phosphorus. Unfortunately even when an excess of ligand was used, only one example of the desired complexes, *mer*-$[Mo(CO)_3(\eta^2\text{-}CH_3N(P(OR)_2)_2)(\eta^1\text{-}CH_3N(P(OR)_2)_2)]$ (R = $CH(CH_3)_2$ (**3**)) could be prepared pure and in good yield, although Cr and W analogues (R = $CH(CH_3)_2$ (**8**, **18**), CH_3, **13**)) were identified spectroscopically as minor products. The primary species obtained in most cases were one or more isomers of $[M_2(CO)_6(PNP)_2(\mu\text{-PNP})]$. Previously, the complexes *fac*-$[M_2(CO)_6(dmpm)_2(\mu\text{-dmpm})]$ have been reported,[32] but this present work appears to be the first instance in which the mer and particularly the fac–mer isomers of complexes of this type have been prepared. It is tempting to attribute the success in obtaining **3** to the bulk of the isopropoxy substituents which might be expected to disfavor formation of a binuclear species (note the discussion of intramolecular nonbonded contacts in **12**) but this explains neither the formation of significant amounts of *mer*-$[Mo_2(CO)_6(L_2')_2(\mu\text{-}L_2')]$ (**2**) when a stoichiometric quantity of the ligand is employed nor the low yield of the mononuclear Cr and W analogues (**8** and **18**) compared to significant amounts of the binuclear species also formed in these latter cases. It may be that the greater ease of substitution of the CHT ligand in $[Mo(CO)_3(CHT)]$ as compared with the Cr and W analogues permits attachment of two ligands to the metal before the uncoordinated end of the monodentate ligand encounters an unreacted (or partially substituted) $[Mo(CO)_3(CHT)]$ species. Steric factors must nevertheless play a part since even with an excess of $CH_3N(P(OCH_3)_2)_2$, only the binuclear species **1** is seen in the molybdenum system.

The ^1H and ^{31}P NMR spectra of the group VI metal complexes deserve comment. With the exception of **7**, the ^{31}P NMR spectra of *mer*-$[M_2(CO)_6(PNP)_2(\mu\text{-PNP})]$ are all second order (*vide supra*). The apparent first-order spectrum for **1** suggests that $J_{11'}$ is essentially zero in this case. It is not obvious why this should be so, but $^2J_{PNP}$ in a variety of $RN(PX_2)_2$ molecules is known to be sensitive to conformation with I having large positive values while

I II

II gives much smaller values, which may even be negative. Observed values for $^2J_{PNP}$ in these species decrease significantly with an increase in the bulk of R but appear to increase somewhat with an increase in the size of X and often show substantial variations with temperature. This has been attributed to varying populations of conformers between the limits represented by I and II.[62–66] Also, $^2J_{PNP}$

(54) Brisdon, B. J.; Edwards, D. A.; Paddick, K. E.; Drew, M. G. B. *J. Chem. Soc., Dalton Trans.* **1980**, 1317.
(55) Bruce, M. I.; Wong, F. S.; Wkelton, B. W.; White, A. H. *J. Chem. Soc., Dalton Trans.* **1981**, 1398.
(56) Bruce, M. I.; Wallis, R. C.; Skelton, B. W.; White, A. H. *J. Chem. Soc., Dalton Trans.* **1981**, 2205.
(57) Consiglio, G.; Morandini, F.; Ciani, G.; Sironi, A.; Kretchmer, M. *J. Am. Chem. Soc.* **1983**, *105*, 1391.
(58) Bruce, M. I.; Humphrey, M. G.; Patrick, J. M.; White, A. H. *Aust. J. Chem.* **1983**, *36*, 2065.
(59) Blagg, A.; Carr, S. W.; Cooper, G. R.; Dobson, I. D.; Gill, J. B.; Goodall, D. C.; Shaw, B. L.; Taylor, N.; Boddington, T. *J. Chem. Soc., Dalton Trans.* **1985**, 1213.
(60) Blagg, A.; Shaw, B. L. *J. Chem. Soc., Dalton Trans.* **1987**, 221.
(61) Blagg, A.; Pringle, P. G.; Shaw, B. L. *J. Chem. Soc., Dalton Trans.* **1987**, 1495, and references therein.
(62) Keat, R.; Sim, W.; Payne, D. S. *J. Chem. Soc. A* **1970**, 2715.
(63) Cross, R. J.; Green, T. H.; Keat, R. *J. Chem. Soc., Dalton Trans.* **1976**, 1423.
(64) Colquhoun, I. J.; McFarlane, W. *J. Chem. Soc., Dalton Trans.* **1977**, 1674.
(65) Bulloch, G.; Keat, R.; Rycroft, D. S. *J. Chem. Soc., Dalton Trans.* **1978**, 764.

tends to be smaller in magnitude when one or both phosphorus atoms is four-coordinate, thus $^2J_{PNP}$ in $CH_3N(P(OCH_3)_2)_2$ is 355 Hz[63] while in its monosulfide the value is 78 Hz.[67] Moreover $^2J_{PNP}$ decreases from over 200 Hz in $CH_3N(P(CH_3)C_6H_5)_2$ to nearly zero in its disulfide, but coordination of a transition metal to phosphorus causes as smaller decrease.[63] From Figure 1, the conformation of the bridging ligand in **12** is closer to II than to I in keeping with the small value observed for $J_{11'}$, and it is reasonable to suggest that in **7** the bulk of the isopropoxy substituents together with the smaller size of chromium enforces a conformation or sets of conformations for the bridging ligand such that the effective value of $J_{11'}$ is essentially zero. This conclusion is reinforced by the observation that $^2J_{PNP}$ (J_{14}) for the monodentate ligand in *mer*-$[M(CO)_3(\eta^2\text{-PNP})(\eta^1\text{-PNP})]$ is considerably smaller when PNP is $CH_3N(P(OCH(CH_3)_2)_2)_2$ (**3**, **8**, **18**) than when it is $CH_3N(P(OCH_3)_2)_2$ (**6**, **13**). Despite the observation (vide supra) that $^2J_{PNP}$ increases with increasing size of X in *free* $RN(PX_2)_2$ molecules, none of the previous studies involved comparisons when one phosphorus atom bore a fourth *bulky* substituent nor was a substituent as bulky as the isopropoxy group used. Since **3**, **6**, **8**, **13**, and **18** comprise a closely related series, it is reasonable to attribute the variation in J_{14} to different conformations of the η^1 ligand with the smaller methoxy substituents permitting a larger population of conformations closer to I.

An interesting feature of the ^{31}P NMR spectra of *mer*-$[M(CO)_3(\eta^2\text{-PNP})(\eta^1\text{-PNP})]$ is an observable coupling between the uncoordinated phosphorus atom (P_4) of the η^1 ligand and that (P_3) in the η^2 ligand which is *cis* to the coordinated end of the former. This is largest in **6** and **14**, where $^2J_{PNP}$ (J_{14}) in the η^1 ligand is also the largest, suggesting that in these complexes the η^1 ligand (L_2) adopts conformations close to I. Indeed, models suggest that with this conformation, an orientation of the η^1 ligand that juxtaposes P_4 and P_3 (III) is not obviously less favorable

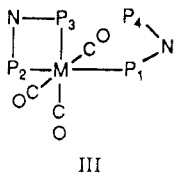

III

than one with the η^1 ligand rotated by ca. 180° about the M–P_2 bond. Using the structure of **12** as a guide, it is entirely possible that in III P_4 could be within 3.5 Å of P_3, suggesting that J_{34} may be a through-space coupling. Although this is rare for phosphorus, a significant through-space coupling has been proposed to occur over a 3.30-Å nonbonded separation.[68] A through-bond mechanism for J_{34} cannot be ruled out, although since this path (P–M–P–N–P) involves the same number of bonds as are involved in the well-documented "virtual" phosphorus–hydrogen coupling when two methyl-substituted phosphines are trans in a metal complex with a large $^2J_{P\text{-}M\text{-}P}$,[69] were it to occur here we might have expected J_{24} to be larger than J_{34} since, at least in **3**, **13**, and **18**, J_{12} is significantly larger than J_{13}. In fact only in **13** is J_{24} detected. In an attempt to distinguish between these two coupling mechanisms, **13** was reacted with a stoichiometric quantity of sulfur. The $^{31}P\{^1H\}$ NMR spectrum of the product (toluene/C_6D_6) showed little change in the chemical shifts for P_1–P_3, but the multiplet originally assigned to P_4 had been replaced by one at 76.6 ppm, which is virtually the same as that for the sulfurized phosphorus atom in $(CH_3O)_2PN(CH_3)P(S)(OCH_3)_2$ (75.0 ppm) indicating that the desired product, *mer*-$[W(CO)_3(\eta^2\text{-}CH_3N(P(OCH_3)_2)_2)(\eta^1\text{-}P(OCH_3)_2N(CH_3)P(S)(OCH_3)_2)]$, had indeed formed. The observed coupling constants are J_{12} = 156.3, J_{13} = 40.5, J_{14} = 18.7, J_{23} = 81.9 Hz. Significantly P_4 is now coupled only to P_1 ($^2J_{PNP}$), and this now much smaller than in **13**. The results, unfortunately, are equivocal. The disappearance of J_{34} on sulfurizing P_4 is certainly consistent with its being due to a through-space process since now the P_3–P_4 distance will undoubtedly be larger. On the other hand, J_{24} could only be a through-bond coupling, and its disappearance is likely the consequence of the significant decrease in J_{14}. If J_{34} were also a through-bond coupling, then the decrease in J_{14} could easily diminish J_{34} below the limit of detectability.

It has previously been shown[30] that $^2J_{PP}$ in *cis*-$[Mo(CO)_4(P(OCH_3)_3)_2]$ and *cis*-$[M(CO)_4(P(CH_3)_3)_2)]$ (M = Cr, Mo, W) is negative and inferred that this is a general feature of complexes of this type. In the complexes reported here, two different cis $^2J_{PP}$ couplings involving the metal occur, most of which can be observed directly. One is that between the chelate and non-chelate ligands and must occur via the metal (J_{13} in the mer complexes), while the other is between the nonequivalent ends of the chelate ligand. The latter coupling will be the sum of that via the metal and that via the ligand backbone.[70] The magnitudes of J_{13} generally decrease as one goes from chromium to tungsten as noted previously,[30] and although we have been unable to determine their signs we do note that in **3** a marginal increase in the agreement between observed and calculated spectra could be achieved if J_{13} is negative. If we assume that $^2J_{PNP}$ through the backbone of the chelate ligand is substantial and positive (conformation I, vide supra), then the fact that the observed magnitudes of J_{23} are smallest in the chromium complexes that have the largest magnitudes for J_{13} suggests that the through-metal contribution to this coupling is also negative, although the data are too variable to draw a firm conclusion.

All the complexes of $CH_3N(P(OCH_3)_2)_2$ show simple doublet resonances for the methoxy protons of the ligands except for **14**, where they appear as a "virtually coupled triplet" as has been observed for its chromium and molybdenum analogues.[10] This implies that $^2J_{P\text{-}P}$ in the chelate ligand of **14** is large, but it is difficult to see why it should be significantly larger than has been observed directly for the same chelate ligand in the other complexes reported here. At present we have no explanation for this.

Where measured, $^1J_{W\text{-}P_1}$ decreases in the order $P_1 > P_2 > P_3$ in *mer*-$[W_2(CO)_6(PNP)_2(\mu\text{-PNP})]$ and *mer*-$[W(CO)_3(\eta^2\text{-PNP})(\eta^1\text{-PNP})]$. The values of $^1J_{W\text{-}P_1}$ compare favorably with those reported for *trans*-$[W(CO)_2(P(OCH_3)_3)_4]$[71] and *trans*-$[W(CO)_4(P(OCH(CH_3)_2)_3)_2]$.[72] Those for $^1J_{W\text{-}P_3}$ are considerably smaller than previously observed for a phosphite ligand trans to carbonyl group[71,72] but are very close to that found in **14**. Possibly this is the result of the distortions of the coordination sphere because of the small bite angle of the ligand. This may also explain why $^1J_{W\text{-}P_2}$ is significantly less than $^1J_{W\text{-}P_1}$ despite the approximately trans disposition of P_1 and P_2.

(66) Bulloch, G.; Keat, R.; Rycroft, D. S.; Thompson, D. G. *Org. Magn. Reson.* **1978**, 12, 708.
(67) Keat, R.; Manojlovic-Muir, L.; Muir, K. W.; Rycroft, D. S. *J. Chem. Soc., Dalton Trans.* **1981**, 2192.
(68) Mathey, F.; Mercier, F.; Nief, F.; Fischer, J.; Mitchler, A. *J. Am. Chem. Soc.* **1982**, *104*, 2077.
(69) Shaw, B. L.; Jenkins, J. M. *J. Chem. Soc. A* **1966**, 770.
(70) Grim, S. O.; Barth, R. C.; Mitchell, J. D.; Delgaudio, J. *Inorg. Chem.* **1977**, *16*, 1776.
(71) Andrews, G. T.; Colquhoun, I. J.; McFarlane, W.; Grim, S. O. *J. Chem. Soc., Dalton Trans.* **1982**, 2353.
(72) Schenk, W. A.; Buchner, W. *Inorg. Chim. Acta* **1983**, *70*, 189.

The heterobimetallic complexes **20–22** are analogous to DPPM species prepared similarly,[61] and as was also noted for $[RhWCl(CO)_4(DPPM)_2]$, **20** is obtained as a mixture of two isomers that interconvert in solution. In contrast to the DPPM complexes, the low-temperature ^{31}P NMR spectrum of **20** clearly shows two species to be present, and we presume that these are **20a** and **20b** as suggested by the X-ray results. We further suggest that these are likely to be the structure adopted for the DPPM complexes as well. Both **21** and **23** are luminescent at low temperature. Details of these results will be reported separately.

[Bis(diphenylphosphino)methyl]-2-pyridine (P_2N) behaves as a tridentate ligand on reaction with $[M(CO)_3(CHT)]$ (M = Mo, W) even when an excess of the ligand is used, and while the pyridyl group can be displaced by carbon monoxide, no reaction appears to occur with more P_2N even under forcing conditions. Attempts to prepare a heterobimetallic complex from $[Rh(P_2N)_2]OTf$ and $[Mo(CO)_3(CHT)]$ were unsuccessful. The only identifiable species in the reaction mixture were the starting rhodium complex and **23**, implying redistribution of the ligand occurred.

Conclusion

Although the ligands $CH_3N(P(OR)_2)_2$ (R = CH_3, $CH(CH_3)_2$, CH_2–) do form dimeric complexes with group VI metals, these are homometallic. Only when R = $CH(CH_3)_2$ can substantial amounts of monomeric species suitable for forming heterobimetallic complexes be obtained. These appear not to be particularly reactive toward small molecules, presumably because of the bulk of the ligands.

Acknowledgment. Financial support of the Tulane University Chemistry Department and the Pennzoil Corp. is gratefully acknowledged. We also thank Professors Max Roundhill, John H. Nelson, and John G. Verkade for helpful discussions.

Supplementary Material Available: Figures S1–S3 and tables of bond distances, interbond angles, anisotropic thermal parameters, amplitudes of anisotropic thermal displacement, calculated hydrogen atom positions, and torsion angles for **12**, **16**, **20**, **21**, and **27** (63 pages); tables of observed and calculated structure factors for **12**, **16**, **20**, **21**, and **27** (151 pages). Ordering information is given on any current masthead page.

Synthesis and Characterization of Five-Coordinate Olefin Complexes of Palladium(II). Molecular Structure of the Acetone Solvate of (2,9-Dimethyl-1,10-phenanthroline)(maleic anhydride)methylchloropalladium

Vincenzo G. Albano* and Carlo Castellari

Dipartimento di Chimica "G. Ciamician", Università di Bologna, via F. Selmi 2, 40126 Bologna, Italy

Maria Elena Cucciolito, Achille Panunzi, and Aldo Vitagliano*

Dipartimento di Chimica, Università di Napoli, via Mezzocannone 4, 80134 Napoli, Italy

Received July 5, 1989

Five-coordinate olefin complexes of palladium(II) of general formula PdClMe(N-N′)(η^2-olefin) have been prepared by reaction of the dimeric complex $[PdClMe(Me_2S)]_2$ with planar sterically crowded nitrogenous bidentate ligands and the appropriate olefin. The X-ray crystal structure of the complex having N-N′ = 2,9-dimethyl-1,10-phenanthroline and olefin = maleic anhydride has been determined. This crystallizes in the monoclinic system, space group $P2_1/n$, with a = 7.085 (2) Å, b = 15.880 Å, c = 19.062 Å, β = 96.79 (5)°, and Z = 4. Refinement converged at R = 0.024 (R_w = 0.026), and the geometry of the five-coordinate palladium is trigonal bipyramidal, with the olefinic double bond in the equatorial plane and the chloride and methyl ligands in apical positions. The stability and structural and NMR spectroscopic properties of the complexes are discussed in comparison with those of analogous Pt(II) derivatives and point to a relevant contribution of π-back-donation to the Pd–olefin bond in the five-coordinate species.

Introduction

In spite of the large number of synthetic reactions involving Pd(II) mono(olefin) complexes,[1] only a limited number of species have been isolated and well characterized.[2,3] Among these, a series of remarkably stable compounds of the type $[Pd(\eta^5\text{-}C_5H_5)L(\eta^2\text{-olefin})]X$ are the only known example of coordinatively saturated species, which could be considered as formally five-coordinate.[3]

During the last few years, a series of contributions from our laboratories has dealt with the synthesis, structural characterization, and properties of five-coordinate olefin complexes of platinum(II),[4–6] giving special attention to

(1) Collman, J.; Hegedus, L. S.; Norton, J. R.; Finke, R. G. *Principles and Applications of Organotransition Metal Chemistry*; University Science Books: Mill Valley, CA, 1987.

(2) Most of the isolated square-planar 16e species belong to the class of the Kharash complexes $[PdCl_2(olefin)]_2$. See for example: Maitlis, P. M. *The Organic Chemistry of Palladium*; Academic Press: New York, 1971; Vol. 1, p 106.

(3) (a) Kurosawa, H.; Majima, T.; Asada, N. *J. Am. Chem. Soc.* **1980**, *102*, 6996. (b) Miki, K.; Shiotani, O.; Kai, Y.; Kasai, N.; Kanatani, H.; Kurosawa, H. *Organometallics* **1983**, *2*, 585. (c) Kurosawa, H.; Asada, N.; Urabe, A.; Emoto, M. *J. Organomet. Chem.* **1984**, *272*, 321.

(4) (a) De Renzi, A.; Panunzi, A.; Saporito, A.; Vitagliano, A. *Gazz. Chim. Ital.* **1977**, *107*, 549. (b) De Renzi, A.; Di Blasio, B.; Saporito, A.; Scalone, M.; Vitagliano, A. *Inorg. Chem.* **1980**, *19*, 960. (c) Albano, V. G.; Demartin, F.; De Renzi, A.; Morelli, G.; Saporito, A. *Inorg. Chem.* **1985**, *24*, 2032.

(5) (a) Albano, V. G.; Braga, D.; De Felice, V.; Panunzi, A.; Vitagliano, A. *Organometallics* **1987**, *6*, 517. (b) Albano, V. G.; Castellari, C.; Morelli, G.; Vitagliano, A. *Gazz. Chim. Ital.* **1989**, *119*, 235.

0276-7333/90/2309-1269$02.50/0